運輸省港湾技術研究所

港湾技術研究所報告

REPORT OF THE PORT AND HARBOUR RESEARCH INSTITUTE

MINISTRY OF TRANSPORT

VOL. 9 NO. 1 MAR. 1970

NAGASE, YOKOSUKA, JAPAN

港湾技術研究所報告　(REPORT OF P. H. R. I)

第9巻　第1号 (Vol. 9, No. 1),　1970年3月 (March 1970)

目　　次 (CONTENTS)

REPORT OF THE PORT AND
HARBOUR RESEARCH INSTITUTE
Vol.9 No.1 (Mar. 1970)

1. Experimental Investigation on the Horizontal Resistance of Coupled Piles

Masatoshi SAWAGUCHI*

Synopsis

In this paper, at first, the several existing methods of computation on coupled piles subjected to a horizontal force at the intersection were outlined. The definition of coupled piles used in this paper will be described later. Next a new method of computation which used the results of load tests or the estimated load-displacement curves on a single vertical pile was proposed.

To comfirm this authenticity, several series of load tests on model coupled piles have been carried out. The model piles for use had a rectangular shape of cross-section and four types of dimensions, composed of 7cm or 10cm in width and the range between 0.9cm and 3.2cm in thickness. Ist to 5th series were to investigate the effect of coupled piles condition, for example, the angle of batter, on the lateral resistance. In 6th series the model coupled piles were tested to collapse so that the lateral behavior to the ultimate resistance might be observed and analyzed from the mechanical point of view.

Particularly, it was emphasized in what percentage the bending resistance in coupled piles was capable to counteract a horizontal force acting at the intersection. A conception "percentage of share" was recommended to express this value and it was described how it varied during application of a horizontal force in increment.

Finally, in Appendix, some existing data about the load tests on the coupled piles carried out in the fields, and the load-displacement relationships with a single pile both in the axial and lateral movements were described for possible reference available to this paper.

* Chief in Foundation Laboratory, Soils Division

港湾技術研究所報告
第9巻第1号（1970. 3）

1. 組グイの水平抵抗に関する実験的研究

沢口正俊*

要　旨

この報告は，これまでに提案され，設計されてきた水平方向力が働らいた時の組グイの計算方法について，まづ述べ，その後室内で行なわれた模型組グイの実験結果について検討した。クイは幅7cmと10cm，厚さ0.9cm～3.2cmの4種類についてである。第1シリーズから第5シリーズまでは，クイの条件を変化させて，各種の要素について，水平抵抗への影響について調べた。第6シリーズでは，組グイの破壊試験を行ない，極限状態に到るまでの組グイの挙動の実験的観察を行ない，その結果の考察を行なった。特に，この報告中では，クイの曲げ抵抗が，どの程度，水平抵抗に寄与し得るかについて重点的に述べてある。この寄与する割合を示す表示法として，分担率という表現方法を採用している。そして，この分担率が，組グイの載荷過程において，どのような変化を示すかについて調べた。

つぎに，組グイの設計法に，いわゆる港研方式を導入して，より精度の高い推定ができるような計算方法を提案した。この計算方法を使って推定した組グイの挙動が，実測値とかなり良い一致を示すことを説明してある。

最後に，現場で行なわれた組グイの載荷実験の結果について概略を集録し，室内の模型実験の結果についての理解を助ける目的に供している。さらに，新しい計算方法の基礎的役割を果たす，クイの荷重・変位関係についてのこれまでの知識を，概略述べてある。

* 土質部　基礎工研究室長

CONTENT

1. Introduction

We can see many cases where piles are used to resist against a horizontal force as a part of foundation in harbour structures. The simplest form of piles for this purpose consists of a single vertical pile, which resists it by its bending and soil reaction. Recently when steel piles with a large diameter have come into wide use, vertical piles are spurred into more utilization. In spite of this fact, if the axial resistance of a pile is made to have its share in a horizontal force, the cross-section might become less. To this end, a batter pile is sometimes used instead of a vertical pile.

If a batter pile inclines towards the force direction, it is called an in-batter pile, and if it inclines to the opposite, an out-batter pile. These two batter piles have different horizontal resistance even if they have other same conditions; the results of the laboratory tests previously carried out showed the fact that the horizontal resistanoe of a batter pile increased as the angle of batter measured from the force direction increased. Therefore, if a single batter pile is subjected to such a force of unforeseen direction as an earthquake, it may not always be more economical to use a batter pile than a vertical pile.

Thus, the top of batter piles including vertical piles are banded together at one point or connected by a slab structure. These types of piles are called coupled piles. However, it is sometimes quite difficult to give such an explicit definition to actual cases; there is a case where it is doubtful whether a pile foundation consists of coupled piles or group batter piles. Therefore, let us define for the present the simplest form of a pile foundation consisting of two batter piles hinged or fixed at their tops ——or the intersection——as coupled piles.

In this paper, the results of load tests on the model coupled piles consisting of an in-batter and an out-batter pile which have the same angle of batter measured from the vertical and the same dimensions, and hinged or fixed together, are described. In these tests a vertical force that corresponds to a dead or live load transmitted from the superstructures was not applied because its action was supposed to influence little upon the horizontal behavior of coupled piles fundamentally.

The principal problem on these fundamental characters of coupled piles is to know what is difference between the axial or lateral behavior of each member——the in-batter or out-batter pile——and of a single pile, and how, if any, such behavior interacts each other in the case of coupled piles.

The first approach to catch these characters is to carry out a series of load tests by changing one pile condition, for example, the angle of batter in coupled piles, keeping constant at all other conditions. It requires a good-controlled uniform testing ground to recognize a little influence by a variation of the pile condition.

In practical design of coupled piles these interacting characters are neglected and its horizontal resistance is assumed to be constituted of the axial and lateral action pertaining to a single pile, or, extremely, to be decided only by the axial bearing resistance of a single pile. In the former, the axial and lateral behavior of a single pile are represented as spring constants and the bending resistance is taken into consideration and, in the latter, it is neglected due to the simplicity in the calculation.

In any event, these two ways are approximate methods and not applicable to accurate displacement determination, even though the above-mentioned interacting characters are elucidated. But this fault can be covered by a new proposed method of computation which will be described in this paper.

2. Methods of Computation on Coupled Piles

The most important point in computation of coupled piles is to know what horizontal resistance can be expected under given site conditions and how much stress occures in these piles. The necessity to know how much displacement at the intersection of coupled piles can be allowed for an available function of the superstructure had not been taken so much seriously. But the coupled piles which are used for a support of a crane-rail or for a foundation of a dolphin which is joined to the land by a girder bridge should require a high accuracy in displacement determination against horizontal forces, for example, ship impact, wave forces or earthquakes. Especially, a relation between the magnitude of an earthquake and the displacement of a structure can become useful data in estimating a degree of damage of sturctures.

As stated before, there are two ways of calculation in coupled piles so far proposed; first, a method of calculation without consideration upon the bending resistance, and second, a method with the consideration upon it. Though it is doubtful whether the second is more reasonable or not, it would usually give an economical pile length.

In the second case, in order to perceive easily how much the bending of piles takes part in the horizontal resistance, a conception "percentage of share" which is defined as

$$\rho=\frac{H_1 \cos \theta_1+H_2 \cos \theta_2}{T} \tag{1}$$

can be useful, where

H_1 and H_2; shearing forces (lateral forces) at the top of the in-batter and the out-batter pile.

θ_1 and θ_2; angles of batter in each pile

T; horizontal force

2.1 Method of Computation Without Consideration upon Bending

It is assumed in this method that any bending moment does not occur in piles under a horizontal force which acts at the intersection. Therefore, the ultimate horizontal resistance of coupled piles is to be determined only by the axial resistance, mostly in harbour structures, by the maximum pulling resistance of the in-batter pile. In the simplest form of coupled piles subjected to a horizontal force as illustrated in Fig.1, the force can be dissolved into two components, N_1 and N_2 paralell to each pile direction, under an assumption that lateral forces, H_1 and H_2, are negligible. Then, the axial forces in each pile can be expressed as

$$\left.\begin{aligned} N_1&=\frac{T \cos \theta_2}{\sin (\theta_1+\theta_2)} \\ N_2&=\frac{T \cos \theta_1}{\sin (\theta_1+\theta_2)} \end{aligned}\right\} \tag{2}$$

Undoubtedly the percentage of share is zero in this case, and so, this method usually overestimates the pile length. However, this has an advantage that its computation is very simple because there is no consideration upon any relation between the load and displacement both in the axial and lateral directions, except when determin-

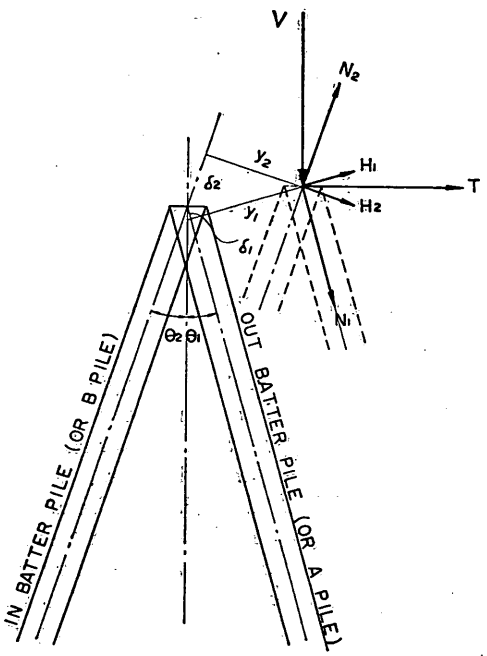

Fig.1 Components of a force at the intersection

ing the displacement at the intersection.

It is true that the lateral force at the top of each pile is negligible in comparision to the axial force, but the fiber stress occured by the moment in the pile is remarkably greater than that occured by the axial force. Therefore, though this method is widely used even at present, there sometimes happens a case that this results in a dangerous determination of the dimensions. In some cases, especially when the free height is relatively large, the axial stress becomes dominent.

2.2 Method of Computation With Consideration upon Bending

It is assumed in this method that an applied force and the induced axial and lateral resistance at the intersection of coupled piles are in equilibrium, and further, the intersected point never breaks off after application of a force. From these conditions, the next four equations can be obtained.

$$\left.\begin{aligned} N_1\cos\theta_1-H_1\sin\theta_1+N_2\cos\theta_2+H_2\sin\theta_2&=0\\ N_1\sin\theta_1+H_1\cos\theta_1-N_2\sin\theta_2+H_2\cos\theta_2&=T\\ \delta_1\cos\theta_1-y_1\sin\theta_1-\delta_2\cos\theta_2-y_2\sin\theta_2&=0\\ \delta_1\sin\theta_1+y_1\cos\theta_1+\delta_2\sin\theta_2-y_2\cos\theta_2&=0 \end{aligned}\right\} \quad (3)$$

where the notations are illustrated in Fig. 1, and the axial force and displacement has plus sign at extension.

As there are eight unknown values in these equations, these are unsoluvable. Hence, if it is assumed that there are some relations between the force and the corresponding displacement, for example, the axial and lateral spring constants at the top of each pile,

$$\left.\begin{aligned} \omega_1&=\frac{N_1}{\delta_1} & \omega_2&=\frac{N_2}{\delta_2} \\ \mu_1&=\frac{H_1}{y_1} & \mu_2&=\frac{H_2}{y_2} \end{aligned}\right\} \tag{4}$$

the equations become determinate.

If, as a simplest case, the two piles have the same spring constants and the same angle of batter, the percentage of share can be expressed so briefly as

$$\rho=\frac{\mu\ \cos^2\theta}{\omega\ \sin^2\theta+\mu\ \cos^2\theta} \tag{5}$$

And the spring constant as the coupled piles becomes

$$K=2\ (\omega\ \sin^2\theta+\mu\ \cos^2\theta) \tag{6}$$

These expressions are obviously independent of the applied force.

The most difficult point of this method in usage is how to establish these unreal spring constants from the load-displacement curves pertaining to a single pile, because the curves never appear in straight lines and still more, they can scarecely be correlated to the soil properties. In fact both the axial and lateral load-displacement curves measured in a load test resemble exponential curves, for these results can be expressed as a straight line on a double logarithmic scale, and so, any well-defined establishment of the spring constant is quite impossible. In Appendix some formulations of the spring constant are explained but their correlation to the soil properties is remained uncertain

2.3 Ultimate Resistance of Coupled Piles

There is a case where it is uneconomical to regard the ultimate horizontal resistance of coupled piles as when the pulling resistance of the in-batter pile reaches the maximum. But the test results described later showed the fact that the horizontal load corresponding to the bending yield of the piles was higher than that corresponding to the maximum pulling resistance of the in-batter pile by 20 percent. This percentage can be easily understood to increase as the flexural rigidity increases comparatively to the peripheral area. In other words it can be said that the maximum pulling resistance will have no relation with the ultimate horizontal resistance of coupled piles whether the flexural rigidity is larger or smaller comparatively to the peripheral area, if that ultimate resistance is defined to be the maximum horizontal resistance achieved before the piles are suffered from a qualitative fault. The qualitative fault of a pile means that the fiber stress attains a yield point. A residual displacement of coupled piles necessarily occures, whether the axial force attains the maximum pulling resistance or not, likewise as in the case of a single pile.

Therefore, in construction of a structure built on coupled piles foundation which is restricted in its displacement, an important problem is not whether the axial force reaches the maximum pulling resistance or not, but whether the piles have a qualitative fault or the displacement at the intersection exceeds an allowable distance or not.

One must know a difference in the degree of dainger between a tension pile and the in-batter pile of coupled piles. A tension pile which is used for a foundation of, for example, a dry dock has a severe condition, because once it attaines the maximum pulling resistance, the dock will collapse. In the other hand, coupled piles keep still

higher horizontal resistance even after the axial force becomes equal to the maximum pulling resistance.

From this point of view, consideration as to the ultimate horizontal resistance of coupled piles should be taken into. Aoki and Kawanishi have proposed the methods of computation in the ultimate horizontal resistance, assuming that the axial and lateral behavior of each pile can be expressed as a broken line including the yield state over the axial bearing resistance, maximum pulling resistance or bending yield. Furthermore, the latter has put forward a conception "percentage of share", which indicates what percentage of a horizontal force acting at the intersection of coupled piles can be resisted by the bending resistance.

2.4 New Method of Computation on Coupled Piles

As stated before, at present it is considered to combine the axial and lateral behavior of a single pile in order to know the behavior of coupled piles subjected to a horizontal force at the intersection. It is true from the test results described later that there is an interacting influence on each other in the axial and lateral behavior of the piles, but as a tentative treatment it cannot help being ignored to make the computation in practice. In this paper a suggestion to the corrective and more accurate procedure for this method will be given.

In the ultimate analysis of coupled piles described before, the load and displacement curves pertaining to a single pile as the basic data in computation are assumed to be represented as broken lines both in the axial and lateral directions. The new method of computation proposed here uses the not modified curves as the basic data for the purpose of more accurate answer in the horizontal behavior of coupled piles. The basic data might be obtained by load tests on a single pile or some estimation formulae on a load and displacement relationship.

In the case of the estimation formulae the same level of accuracy should be required for establishing both the relationships. If such a non-linear expression in the axial load and displacement relationship as exemplified in Appendix is to be used, the Kubo's method should be used properly for the lateral relationship. The new method has an advantage in giving the more correct answer, if the more accurate expressions are used as the basic data of a single pile behavior.

For explanation of the new method of computation, let us assume that these curves are given as illustrated in Fig.2(a), where N_1 curve expresses a load-settlement curve as the out-batter pile, N_2 curve expresses a pull-rise curve as the in-batter pile, H_1 curve and H_2 curve express the lateral load and displacement curves respectively. The downward pile resistance is generally higher than the pulling resistance, and keeps in increment or, at least, becomes constant as the penetration progresses. On the other hand, the pulling resistance decreases after the maximum value is reached. On the lateral relationships the in-batter pile has generally higher resistance than the out-batter pile.

If it is assumed as shown in Fig.2(b) that the intersection of the coupled piles O is translated to the position F under a horizontal force, this displacement can be dissolved into two components, the axial and lateral displacements, in both of the in-batter and the out-batter pile respectively. As the point F is indeterminate, the axial component of displacement can be taken as the same δ_0 between the two

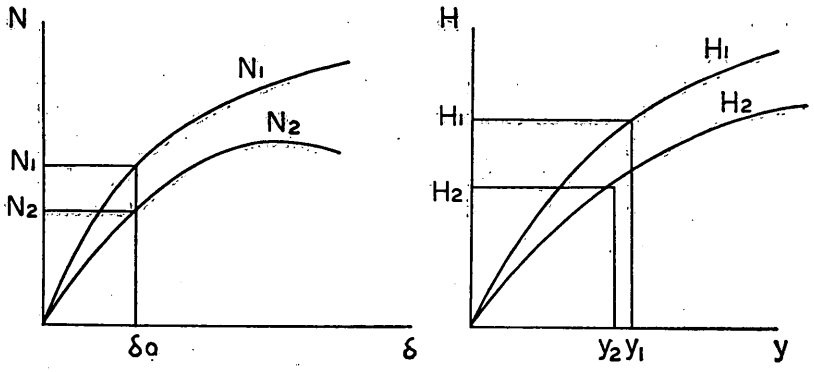

Fig.2(a) Load-displacement curves

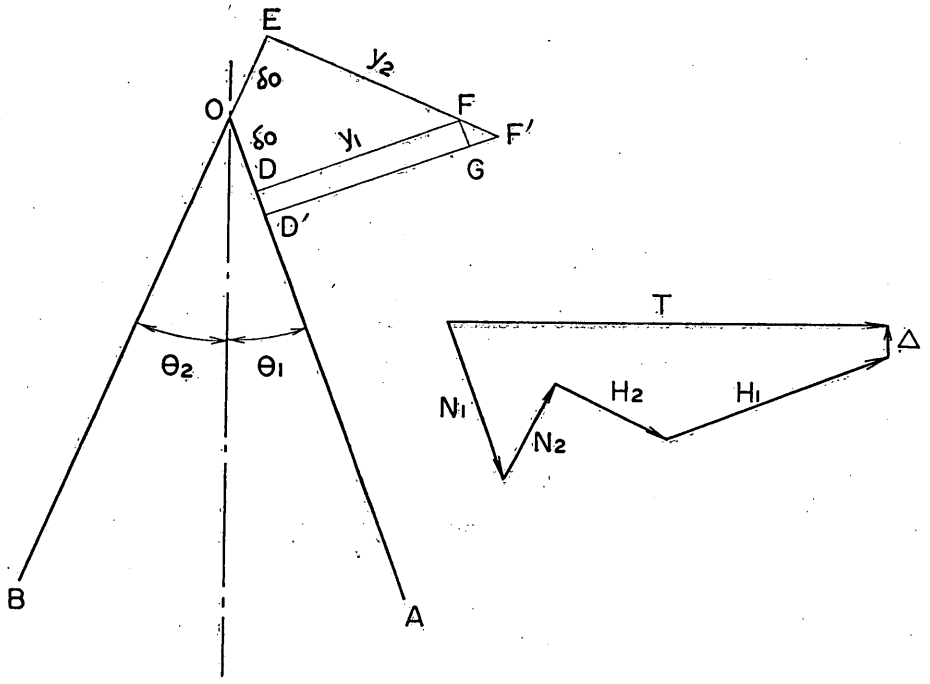

Fig.2(b) Translation of the intersection

piles as the first trial. The axial forces corresponding to those axial displacements can be picked from Fig. 2(a) as N_1 and N_2. And F can be determined by drawing the straight lines perpendicular to the direction of the pile shafts as an intersecting point. This gives the lateral displacements as y_1 and y_2, and then the corresponding lateral forces H_1 and H_2.

As a vertical force is not applied in this case, the sum of vertical components

of these forces should be zero, but generally some remainder will exist. Let us signify this remainder as Δ, and it can be expressed as

$$\Delta=N_2\cos\theta_2+H_2\sin\theta_2-(-N_1\cos\theta_1+H_1\sin\theta_1) \tag{7}$$

where the sign of forces are conformed to the rule mentioned before. The algebraic meaning of the remainder is illustrated in Fig.2(b).

In order to make Δ zero, N_1 is corrected with an addition by

$$\Delta N_1=-\frac{\Delta}{\cos\theta_1} \tag{8}$$

which results in compression of the in-batter pile by DD′. As a result, the translated intersection is also shifted to the point F′. By this correction procedure, the axial and lateral displacement of the out-batter pile and the lateral displacement of the in-batter pile will change, and the corresponding axial and lateral forces should be picked again from Fig.2(a). By substituting these corrected forces into Eq.7, Δ which will be closer to zero can be calculated. If Δ is not negligible, the above-mentioned corrective computation should be repeated. In general, the repetition can be twice or third times, but as the translation increases, it will become more. The remainder less than 1 percent of the axial force can be considered to be satisfactory.

By using these finally corrected values, the horizontal force applied, the corresponding vertical and horizontal displacement T, X, and Y can be calculated as

$$\left.\begin{aligned} T&=-N_2\sin\theta_2+H_1\cos\theta_1+N_1\sin\theta_1+H_2\cos\theta_2\\ X&=\delta_2\cos\theta_2+y_2\sin\theta_2=\delta_1\cos\theta_1-y_1\sin\theta_1\\ Y&=-\delta_2\sin\theta_2+y_2\cos\theta_2=\delta_1\sin\theta_1+y_1\cos\theta_1 \end{aligned}\right\} \tag{9}$$

And with the use of these values the percentage of share can be also obtained by substituting into Eq.1. The stress in the piles can be determined as a combination of the axial stress induced by the axial forces and the fiber stress induced by the bending moment.

After the completion of the first step of repetitive computation, the first assumed axial displacement δ_0 will be increased to the next step.

It is possible to take N_2 as a variable for correction, but, as the N curve descends generally after the maximum pulling resistance, the corrected N sometimes has an imaginary quantity.

In case where a constant vertical force acts at the intersection of coupled piles during application of a horizontal force in increment, the initial state can be determined under an assumption that a vertical force could be supported only by the axial resistance, because the deformation of coupled piles by the weight of a superstructure may be negligible in comparision with that by a horizontal force in harbour construction.

3. Model Tests

3.1 The Plan of Experiments

Lateral load tests were carried out on model coupled piles consisting of two batter piles. Among the factors influencing the lateral resistance of coupled piles,——as to each member——the rigidity of a pile, the height of load application, the embedded length,——as a coupled system——the angle of batter and the fixity of intersection are considered in this paper. Principal features of the model tests are given in

Tab.1 Principal features of the model tests

VARYING FACTOR	h	THICK-NESS	WIDTH	LENGTH	θ	SPRING CONST.	MEMO.
angle of batter θ	25cm	1.2cm	7cm	170cm	10°	4.0kg/cm	
	〃	〃	〃	〃	〃	〃	
	〃	〃	〃	〃	15°	80	
	〃	〃	〃	〃	20°	130	
	〃	〃	〃	〃	25°	160	
	〃	〃	〃	〃	10°	25	
	〃	〃	〃	〃	〃	35	fixed
	44	0.9	10	270	11°	240	
	42	〃	〃	〃	25°	350	
	38	1.9	〃	〃	5°	25	
	45	〃	〃	〃	10°	80	
	47	〃	〃	〃	19°	160	
	41	3.2	〃	〃	12°	180	
	42	〃	〃	〃	21°	370	
	45	〃	〃	〃	20°	220	
rigidity	44	0.9	〃	〃	11°	240	
	45	1.9	〃	〃	10°	80	
	41	3.2	〃	〃	12°	180	
	47	1.9	〃	〃	19°	150	
	42	3.2	〃	〃	21°	370	
	45	〃	〃	〃	20°	250	
height of load application h	25	1.2	7	170	10°	40	
	96	〃	〃	〃	〃	〃	
	20	〃	〃	〃	〃	〃	
	20	〃	〃	〃	20°	100	
	25	〃	〃	〃	〃	130	
	49	〃	〃	〃	〃	〃	
	96	〃	〃	〃	〃	〃	
embedded length l	42	0.9	10	270	25°	350	
	47	1.9	〃	〃	19°	150	
	42	3.2	〃	〃	21°	400	
	45	1.2	7	170	20°	80	

Tab.1, and the types of tests are described in Tab.2.

Pulling tests were made for comparision between the axial behavior of members of coupled piles and that of a single pile. In the case of group piles, especially coupled piles, pile spacing is not wide. Behavior of each member subjected to an external force has, therefore, influence upon each other. In these series, effects of pile spacing on lateral resistance were studied briefly.

Tab.2 Description of tests

SERIES	PILE.No	MEMBER A	MEMBER B	EI(kg.cm²)	θ	h(cm)	T_{max} (kg)	ΔT(kg)	MEMO.
1	CP— 1	NP— 8	NP— 7	2.117×10^6	10°	25	320	20	
	CP— 2	NP— 3	NP— 2	〃	15°	〃	360	〃	
	CP— 3	NP— 5	NP— 6	〃	20°	〃	400	〃	
	CP— 4	NP— 4	NP— 1	〃	25°	〃	460	〃	
2	CP— 1	NP— 8	NP— 7	〃	10°	20	240	〃	fixed intersection
	CP— 2	NP— 2	NP— 3	〃	20°	20	360	〃	〃
	CP— 3	NP— 1	NP— 4	〃	10°	96	60	〃	
	CP— 4	NP— 5	NP— 6	〃	20°	〃	220	〃	
3	CP— 1	PP— 6	PP— 7	1.276×10^6	11°	44	240	20	
	CP— 2	PP— 9	PP— 8	12.00×10^6	5°	38	480	60	
	CP— 3	PP—10	PP—11	57.35×10^6	12°	41	600	〃	repeated 5cycles
4	CP— 1	PP— 6	PP— 7	〃	25°	42	780	60	
	CP— 2	PP— 9	PP— 8	〃	19°	47	720	〃	
	CP— 3	PP—11	PP—10	〃	21°	42	900	〃	
5	CP— 1	PP— 9	PP— 8	12.00×10^6	10°	48	400	40	
	CP— 2	PP—10	PP—11	57.35×10^6	20°	45	480	〃	
	CP— 3	NP— 3	NP— 4	2.117×10^6	20°	〃	160	20	
6	CP— 1	NP—13	NP— 5	2.117×10^6	10°	25	450	10～40	
	CP— 2	NP— 7	NP—11	〃	〃	〃	690	20	
	CP— 3	NP—14	NP—15	〃	〃	〃	590	20～40	fixed intersection
	NP—8 & NP—12			〃	PULLING TEST				
TESTS ON PILE SPACING									

3.2 Test Procedures

3.2.1 Loading

a) Coupled piles

The load-control method was adopted. A horizontal tensile load was in increment applied statically to the piles at the intersection by means of a device consisting of a cable, pulleys, and weights as shown in Fig.3. The maximum load and the load increments in every pile test are shown in Tab.2. At every load stage, one load was kept constant until the rate of deflection became 0.01 mm/min. (after yielding, 0.03 mm/min.).

b) Axial loading test

Axial loading test was carried out on a single vertical pile, where a load was applied through a proving ring by means of screw-jack reacting against a H-beam

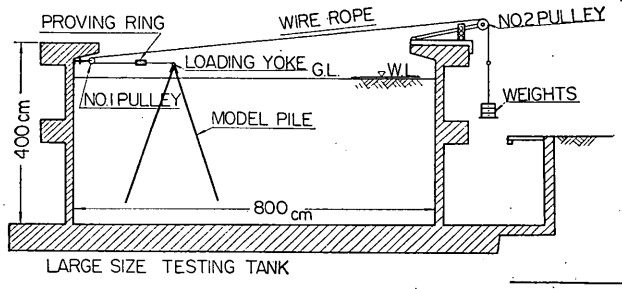

Fig.3 Testing equipment

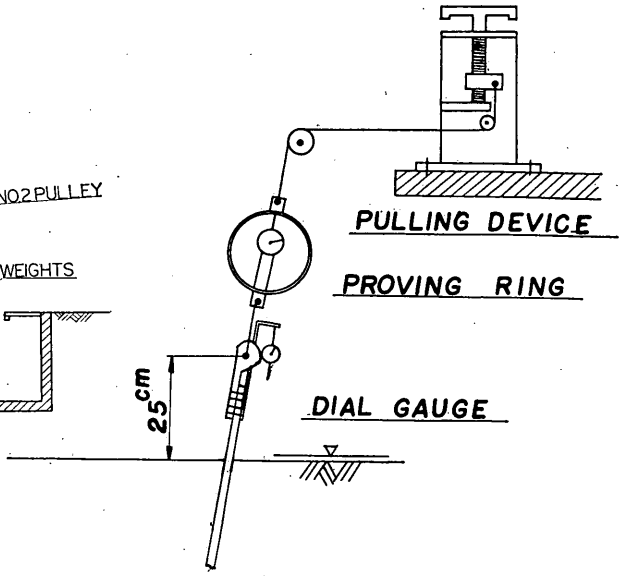

Fig.4 Pulling test procedure

which in turn was fixed at the side walls. Each settlement was maintained for a minimum of 5 minutes or until the rate of load decrement was reduced to 0.2 kg/min..

Axial load was measured at 0 sec., 20 sec., 40 sec., 1 min., 1.5 min., 2 min., 3 min., ……after loading in each step.

c) Pulling tests

The displacement-control method was adopted, in which pull increasing step-wise was applied to the pile top with the pulling device such as shown in Fig.4. A rise was kept constant until the rate of load decrement became 0.1 kg/min.. Loading was continued until the maximum load was exceeded.

d) Tests on pile spacing

Two vertical piles were placed at intervals of 10 to 50cm (1.5B to 4B). A load was first applied to the fore pile, increasing step-wise, and the load was fixed at some value (T_1). Another load (T_2) was then applied in increment to the back pile, with a measurement in the influence of the back pile on the fore pile. (see Fig.5) The loading procedure is the same as a). Equilibrium condition is 0.01 mm/min.

3.2.2 Measuring

a) Applied load

A horizontal tension applied to the model pile was measured by means of a proving ring which has the maximum measuring capacity of 1 ton set between the model piles and the first pulley. Reading was determined after equilibrium was achieved.

b) Displacement

1) Horizontal displacement at the piles intersection was determined with a steel rule fixed horizontally and in the load direction.

2) Deflection was measured with dial gauges (stroke and reading are 80 by 0.1 mm) at four points. The pins of gauges touched directly the pile surface as shown in Fig.6, and only the out-batter pile in 6th series, the metal fittings to set gauges was

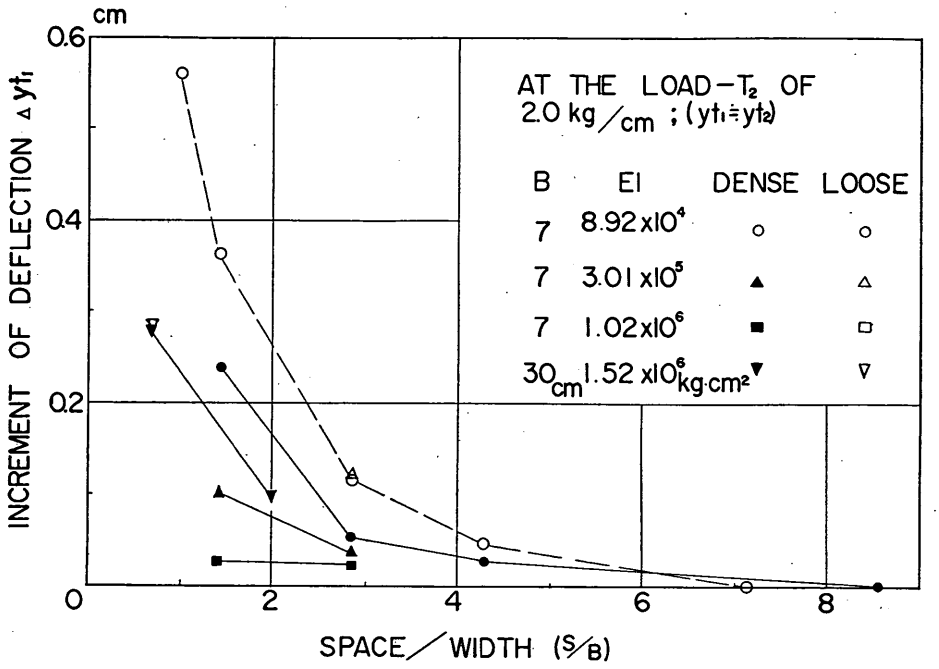

Fig.5 Result of pile spacing

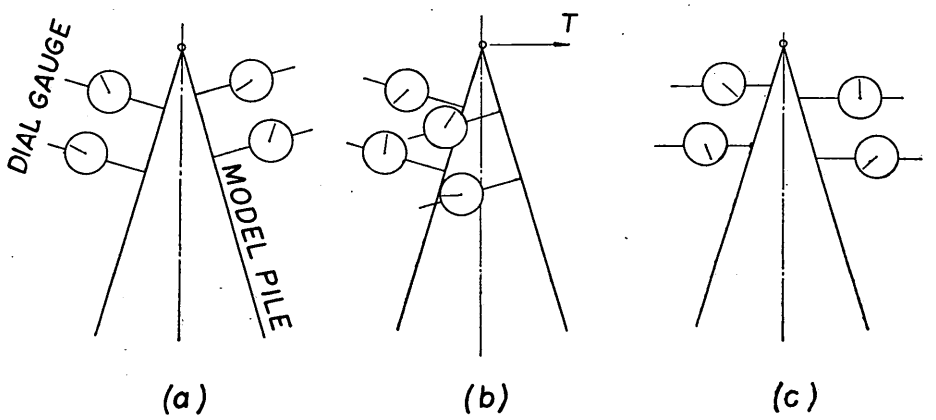

Fig.6 Attachment of dial gauges

attached. These four results yield the horizontal and vertical displacements 1), 3). For one gauge, deflection increment was read at 0 sec., 20 sec., 40 sec., 1 min., 2 min., 3 min.·····after loading in every step. Time for waiting was 4~30 minutes per one step in lst~5th series and 4~200 minutes in 6th series.

3) Vertical displacement was determined with a tilting level only in 6th series. The metal fitting of the piles intersection is circular (see Fig.7). Survey was there-

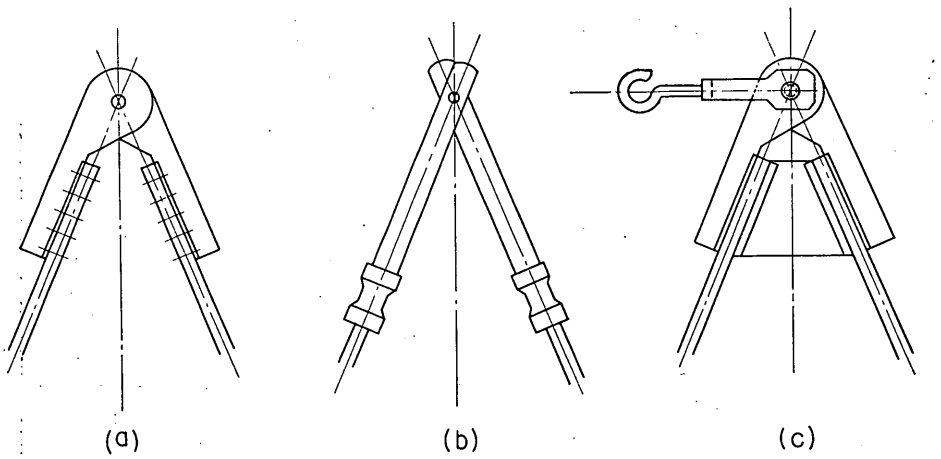

Fig.7 Connection at the intersection

fore performed for a steel rule (2 meter long graduated by 1 mm) placed at the pile top. The accuracy of this measurement is much lower than 2).

c) Pile surface strain

In order to make the behavior of pile-soil system subjected to a static lateral load clear, pile surface strains were measured by means of wire strain gauges. Reading was performed with a static strain indicator (PS-7LT) and a switch box (PS7-100S). The measurement values by two-gauge method and one-gauge method yield the bending strain and the axial strain respectively.

Measured strain data were corrected by checking with its distribution and relationship between a load and strain on the basis of one-gauge measurement and two-gauge measurement data. Distribution of the bending moment induced in a pile was obtained from the above results (strain).

The first and the second differentiations of a moment curve give share and soil reaction, and the first and the second integrations give inclination and deflection of the pile, respectvely. These operations were performed numerically, for lst to 5th series. For 6th series, a moment curve was approximated to a polynominal of the 15th order by the least squares method, and differentiation and integration of this approximate function were made analytically by a computor.

d) Deformation of ground surface was measured with the eye.

3.3 Testing Apparatus

a) Model piles

As model piles, steel plates which have rectangular cross-section were used. In order to measure the (pile) surface strain, wire-strain gauges were used. Steel was taken as pile material, because it is homogneous and it is easy to attach and maintain strain gauges on it. Model must insure the similarity to prototype. From this point of view, the reducing rate of lst to 2nd higher order is required for EI of a pile than

for the cross-sectional area. Rectangular cross-section having a small moment of inertia was taken in the experiments as mentioned above.

The wire-strain gauge used here is polyester gauge, 10mm in gauge length and has gauge factor of 2.05 to 2.10, gauge resistance of 120Ω. Wire strain gauges were attached on both sides of the piles at 15 to 30 levels, 5 to 10cm apart. Every gauge was bonded with polyester resin adhesives (PC-12), and coated with bleached cotton cloth steeped polyester resin (Rigolac).

The angle of friction between the coated pile and sand is 35 degrees from the sliding tests. In these tests a pile was laid on the test sand and pulled to measure the surface friction under application of some weight.

A calibration was conducted for all model piles in order to investigate the pile property for bending and response of wire-strain gauges. A line load in increment was applied to a model pile supported as a simple beam at the middle of the span by means of calibrated weights. After each load increment, the deflection and the bending strain were determined.

b) Testing apparatus

All loading on the coupled piles were conducted in a large size testing tank. It is reinforced concrete container, 8m long, 4.5m wide, and 4m deep, having counterfort walls. It has five basins in the right and left sides, respectively. These are connected with the testing tank by a large number of water holes which have filters, 5cm in diameters. Tests on pile spacing were coducted in a half part of a small size testing tank, 3.5m long, 2m wide, and 1.65m depth.

Three types of metal fitting were used for piles intersection (see Fig.7). B-type was used for CP-1, CP-2 and CP-3 in 3rd series. C-type was used for CP-1 and CP-2 in 2nd series and CP-3 in 6th series. A-type was used for others.

3.4 Model Subgrade

3.4.1 Sand properties

As material of the subgrade, Sagami sand (medium-size river sand) was used for lst to 6th series tests, and Takahagi sand (medium-size clean beach sand) for tests on pile spacing. Their grain size distributions are shown in Fig.8. Some physical properties of the sand are summerized in Tab.3.

3.4.2 Subgrade conditions

a) Making of the model subgrade

Loose sand is 1) in unstable state, 2) not uniform in density, 3) easy to disturb at the surface of layers, and when the similarity between prototype piles and the model piles are considered, 4) dense sand is able to decrease the reducing rate of flexural rigidity (EI) of the pile. Because of the reasons above-mentioned, high density was chosen as the object. 5 to 6 coupled piles were placed in the testing position in the tank, the material sand was filled. Compaction was then performed following the rigidly standarized procedure. This procedure was determined after the preliminary test (see Ref.14).

That is, 1) one finished layer is 20cm thick, 2) after water level was raised 10 to 20cm higher than every fixed finishing level, sand was filled 4 to 5cm higher than the finishing level, 3) under water level, the surface of sand layer was made even and horizontal, 4) water level was let down 40cm lower than the finishing level, and

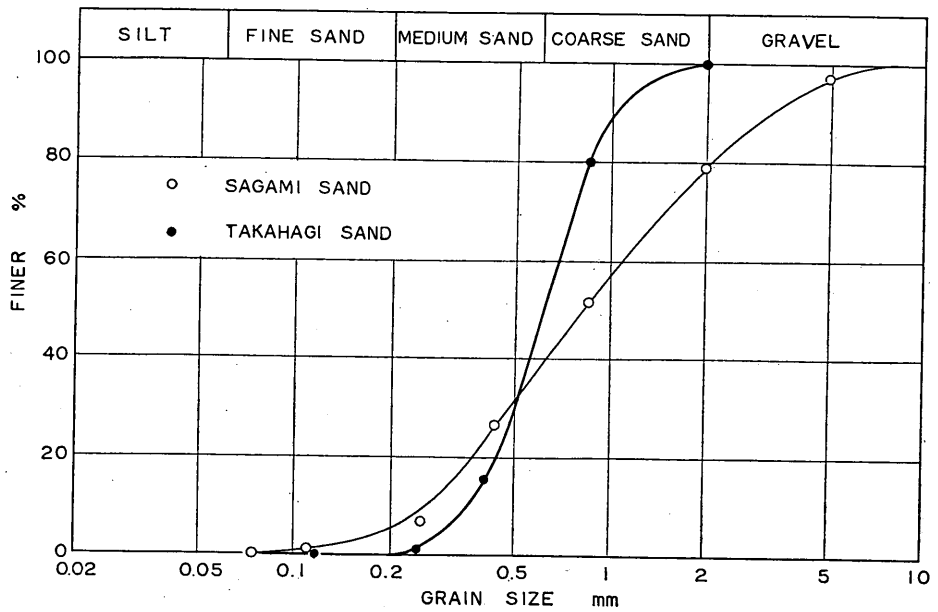

Fig.8 Grain size distribution

Tab.3 Physical properties of sand

DESCRIPTION	SAGAMI SAND	TAKAHAGI SAND
EFFECTIVE SIZE (D_{10})	0.27mm	0.35mm
UNIFORMITY COEFFICIENT (U)	4.15	2.11
SPECIFIC GRAVITY (Gs)	2.675	2.668
MAXIMUN DRY DENSITY (γ_{dmax})	1.96g/cm³	——
MINIMUM DRY DENSITY (γ_{dmin})	1.12g/cm³	——
RELATIVE DENSITY (Dr)	86.5%	——
(MODIFICATION OF BULKING EFFECT)	(64.7)	
ANGLE OF INTERNAL FRICTION (Φ)	44°	39°
	(γ_d=1.76)	(γ_d=1.68)

maintained at the level for 10 minutes, 5) the layer was compacted by hand tampers. The tamper is 8.3kg in weight and has the base 30×30cm. It was let fall naturally from 25cm height 8 times in every 900 cm² area.

b) Subgrade conditions

After the loading tests were finished, the dry unit weight of the model subgrade was determined by means of the funnel and jar method in lst to 6th series. For all of these series, the dry density of model subgrade was controlled to become 1.76± 0.06g/cm³. The angle of internal friction at this density (the relative density of 88%)

is 45° from triaxial compression tests and cohesion is zero.

Some kind of sounding tests were performed on these saturated subgrade. Those are the standard penetration test and two kinds of dynamic cone penetration test. The results of the sounding tests are plotted in graphs as represented by Fig.9 to Fig.11.

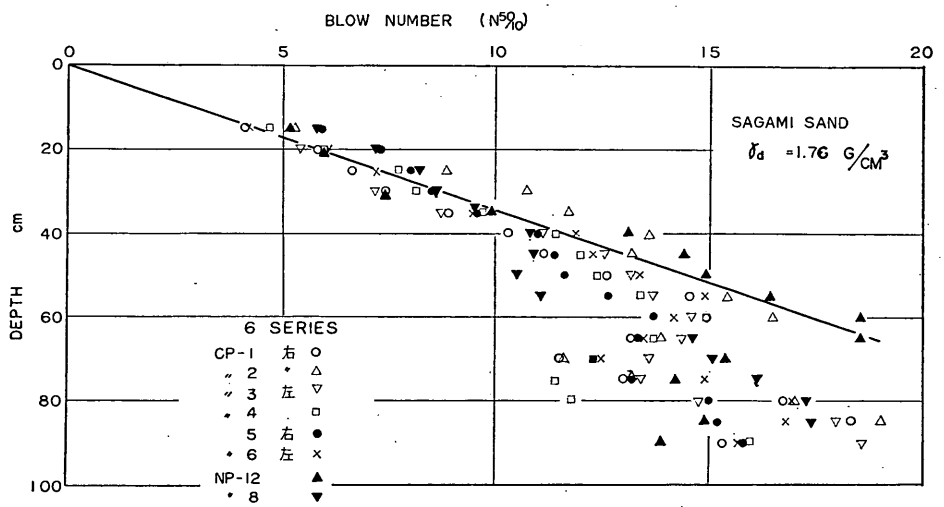

Fig.9 Dynamic cone penetration test result on Sagami sand

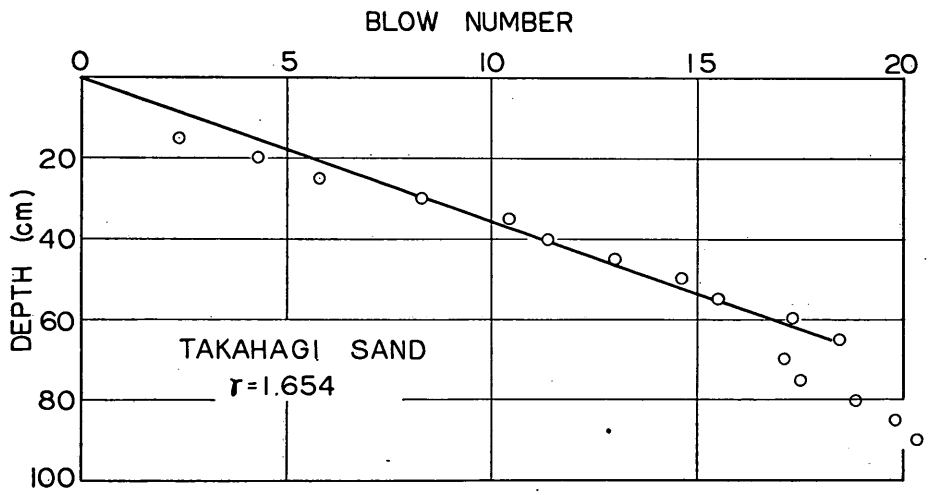

Fig.10 Dynamic cone penetration test result on Takahagi sand

The sounded subgrade strength increases linearly with depth within 60 to 80cm below ground surface, and remains almost constant throughout the depth below this level. The dominant depth in the lateral resistance problem is $(1/4\sim1/3)l_{m1}$. Only the soil within the range down to $(1\sim0.5)l_{m1}$ is important. This depth is 30

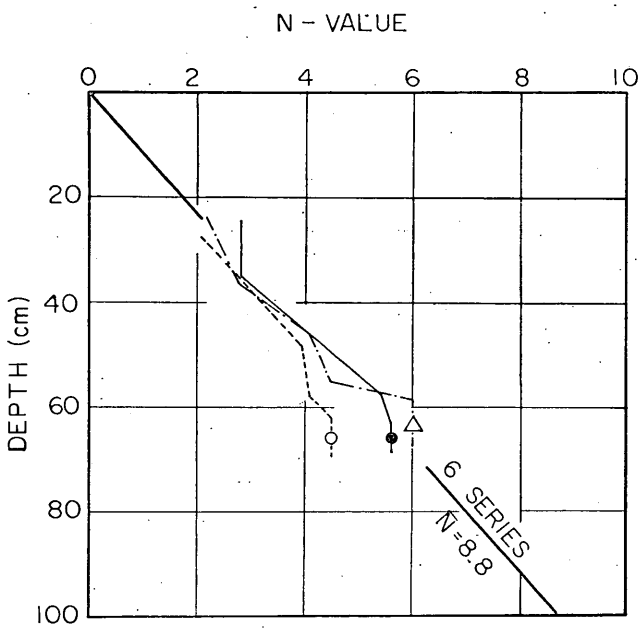

Fig.11 Relationship between depth and the N value

to 80cm for NP-piles and PP-piles in the subgrade. The model subgrade in all series is therefore regarded as S-type soil. $\tilde{N}$ is 8 to 12 and the corresponding k_s is 17 to 65g/cm$^{3.5}$. $\tilde{N}$ means the value of N at a depth of 1m, when actual distribution of N is represented by a straight line starting from zero at the surface.

4 Discussion on the Model Test Results

When coupled piles are applied with a horizontal force at the intersection, it is deflected likewise as other type of piles.

Fig.12 shows the typical curves of a horizontal force and displacement at the intersection of the coupled piles in lst series. After a certain maximum force is reached, the force is released. An estimated relation curve in the case of double vertical piles are added for reference. These curves correspond to four kinds of coupled piles which have angles of batter of 10°, 15°, 20° and 25° having the same other conditions. The solid line representing the out-batter pile and the dotted line representing the in-batter pile should have coincided substantially. This difference seems due to an error on measurement of dial gauges.

The effect of the angle of batter upon the horizontal resistance can be found out to be remarkable from this graph; that is, the larger the angle of batter, the higher the horizontal resistance of the coupled piles.

In 6th series where two tests on hinged-head coupled piles and one on fixed-head coupled piles were carried out, it was investigated how these coupled piles behaved when they were loaded horizontally to a great extent beyond the load intensity cor-

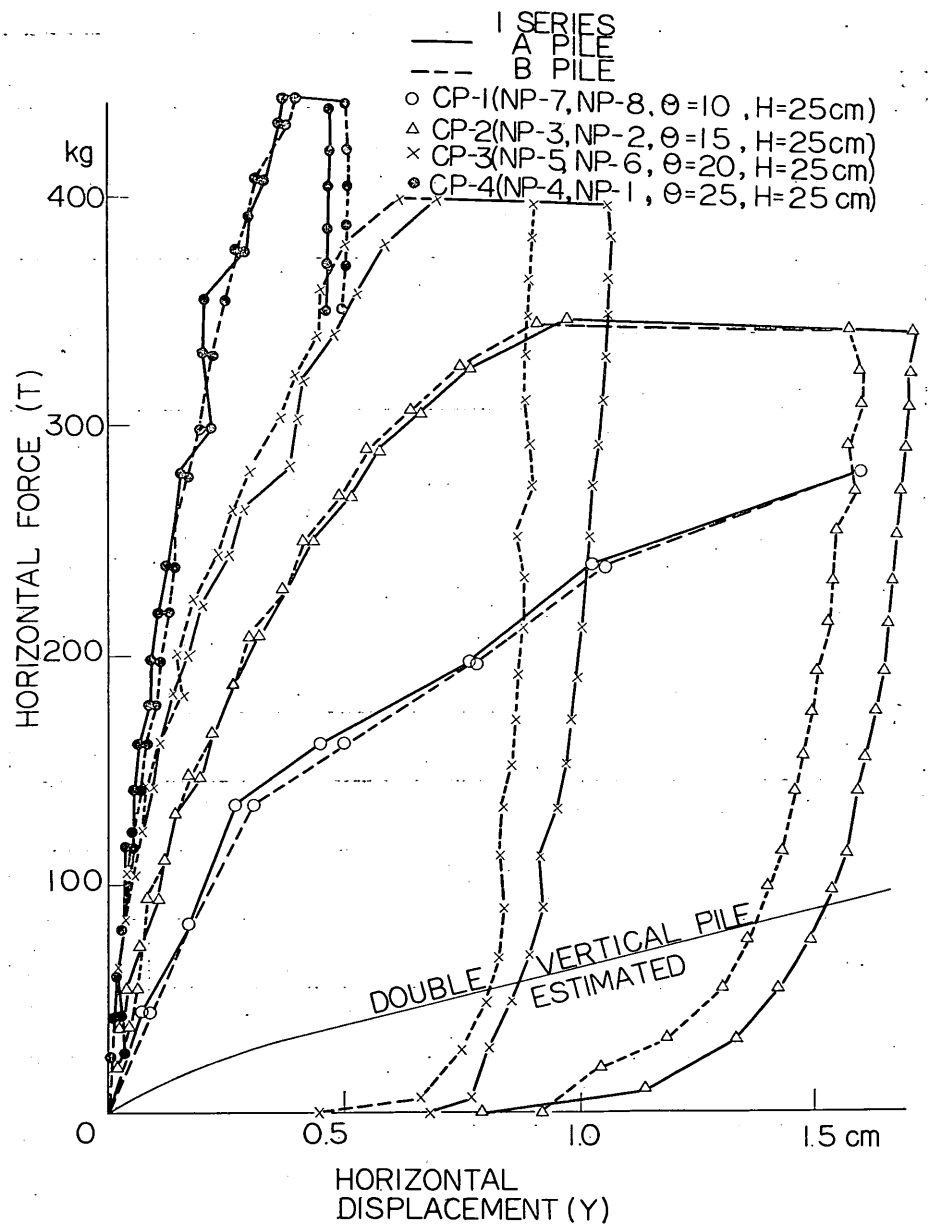

Fig.12 Horizontal force and displacement curves (lst series)

responding to the maximum pulling resistance of the in-batter pile. Fig.13 to Fig.15 show all the results of these series. The load intensity in lst cycle is limited within the elastic range, and in 2nd cycle the load was applied to a considerable extent.

From these diagrams it is obvious that the horizontal resistance never de-

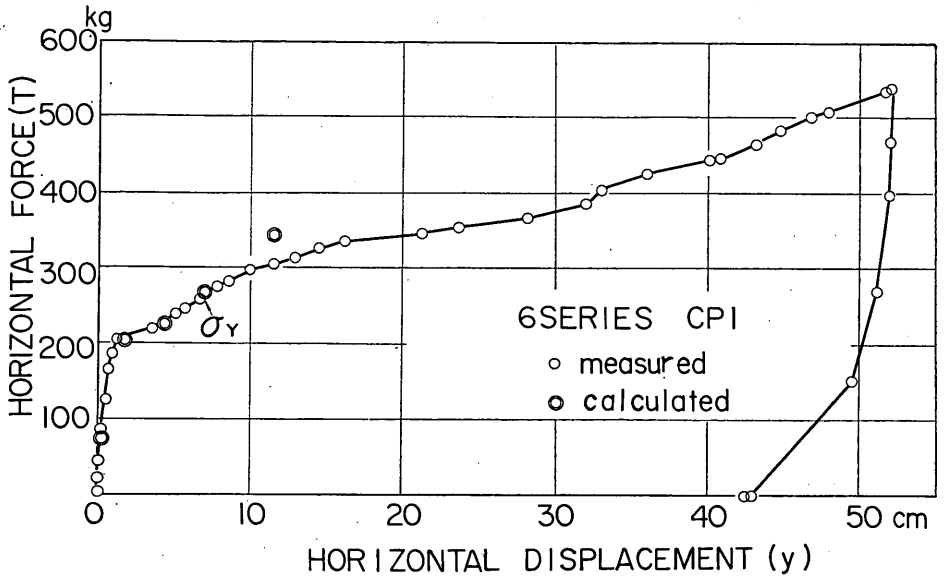

Fig.13 Horizontal force and displacement curve (6th series, CP-1)

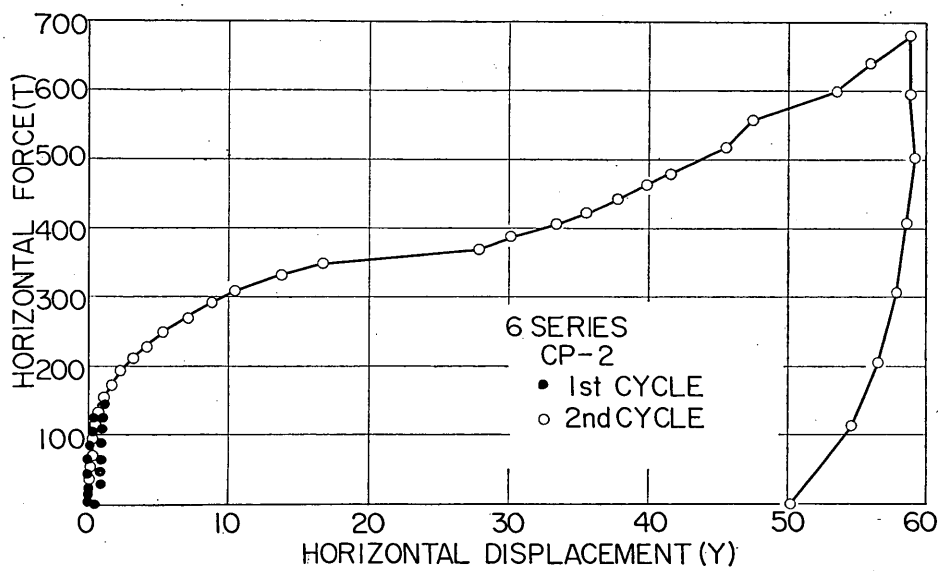

Fig.14 Horizontal force and displacement curve (6th series CP-2)

creases during the loading. σ_y in Fig.13 indicates the point where the fiber stress of the piles attained a yield value (σ_y=3200kg/cm$_2$). This yield value was obtained by an extension test of a steel piece. And double open circles indicate the result estimated by the new method of computation on the basis of the data with respect to

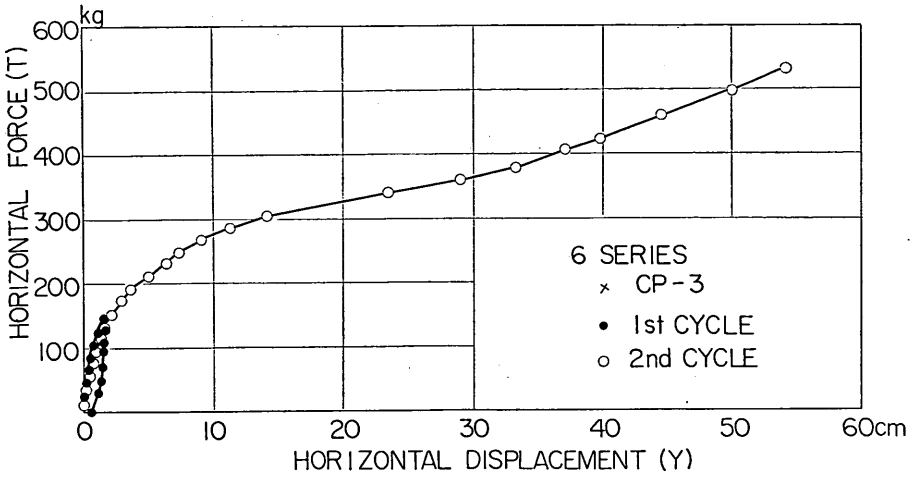

Fig.15 Horizontal force and displacement curve (6th series CP-3)

the axial and lateral behavior of each member of these coupled piles.

The effect of the fixty at the intersection of the coupled piles upon these curves exist, if ever, not distinctly in so far as the horizontal force and displacement relationship is concerned. From these graphs in 6th series, it is obvious that the horizontal resistance of the coupled piles can be held to a considerable extent beyond the bending yield of the piles, although the displacement becomes remarkable.

To make clear the effect of the angle of batter upon the horizontal resistance, the secant modulus which can be obtained from a straight line intersecting the curve at one-half the applied maximum force, was plotted against the angle of batter as representing a spring constant of the coupled piles, as shown in Fig.16.

The advantage of use of the secant modulus is considered to be a quantitive comparision with all these results from a definite standard of judgement.

In addition to the spring constants obtained from Fig.12, those of the coupled piles in other series that have the different piles condition were compared in variations with the angle of batter. All of these curves can be noticed to have the same tendency as lst series, and furthermore, the slopes of these curves appear to be almost the same. This graph expresses the result that the spring constant of the coupled piles with smaller flexural rigidity is relatively larger at the same angle of batter, but this seems not to be in reality.

Besides the effect of the angle of batter, the height of load application was varied under the same other conditions in order to see its effect upon the horizontal resistance of the coupled piles. The results are illustrated in Fig.17. In this graph the spring constants at the angle of batter of 10°and 20°are compared. In both angles of batter, the effect of the height of load application can not be discerned at all.

Fig.18 shows the effect of flexural rigidity upon spring constants. In this graph the tendency appeared in Fig.16 is also involved as a descendant part. But as a whole any definite tendency cannot be recognized.

The effect of embedded length of the coupled piles upon the spring constants shown in Fig.19 is also indistinct because, perhaps, of the scant data.

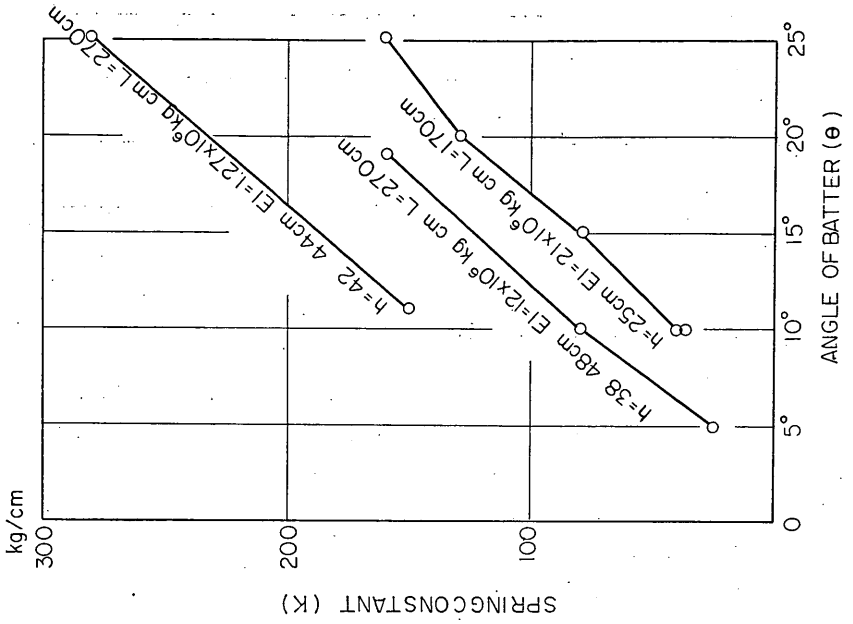

Fig.16 Influence of angle of batter upon spring constant

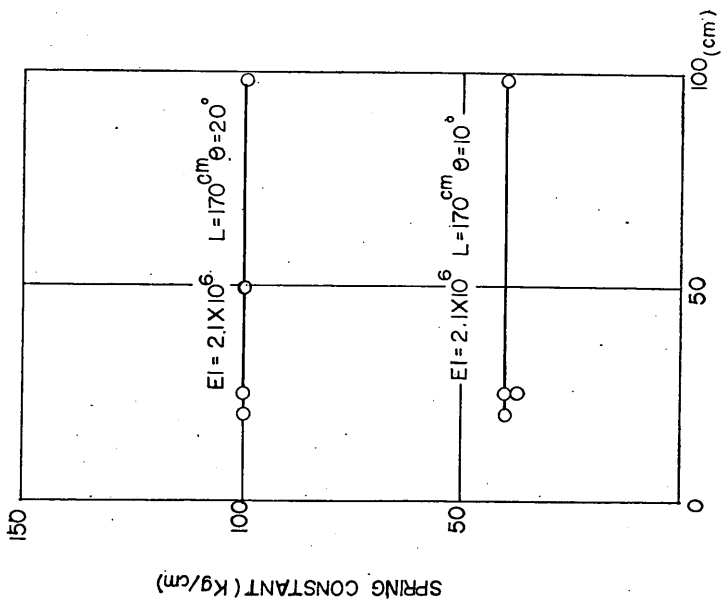

Fig.17 Influence of height of load application upon spring constant

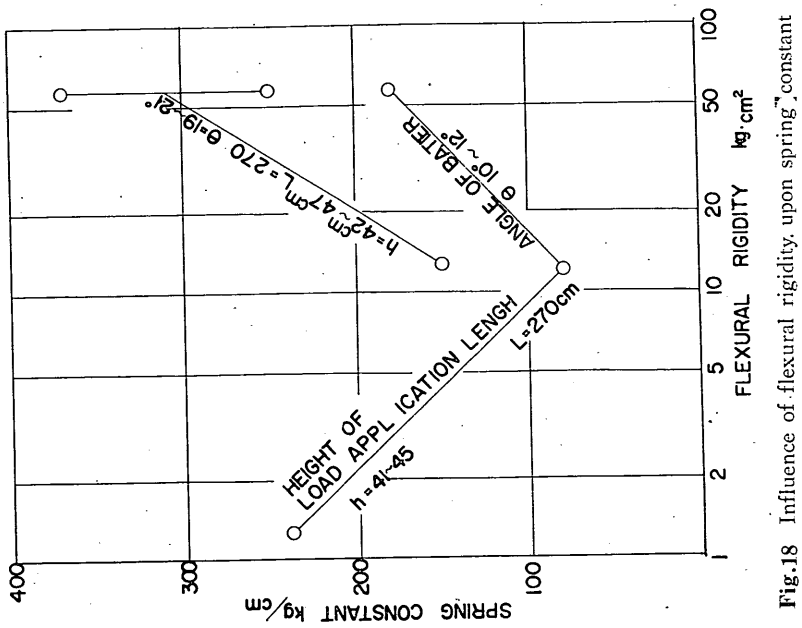

Fig.18 Influence of flexural rigidity upon spring constant

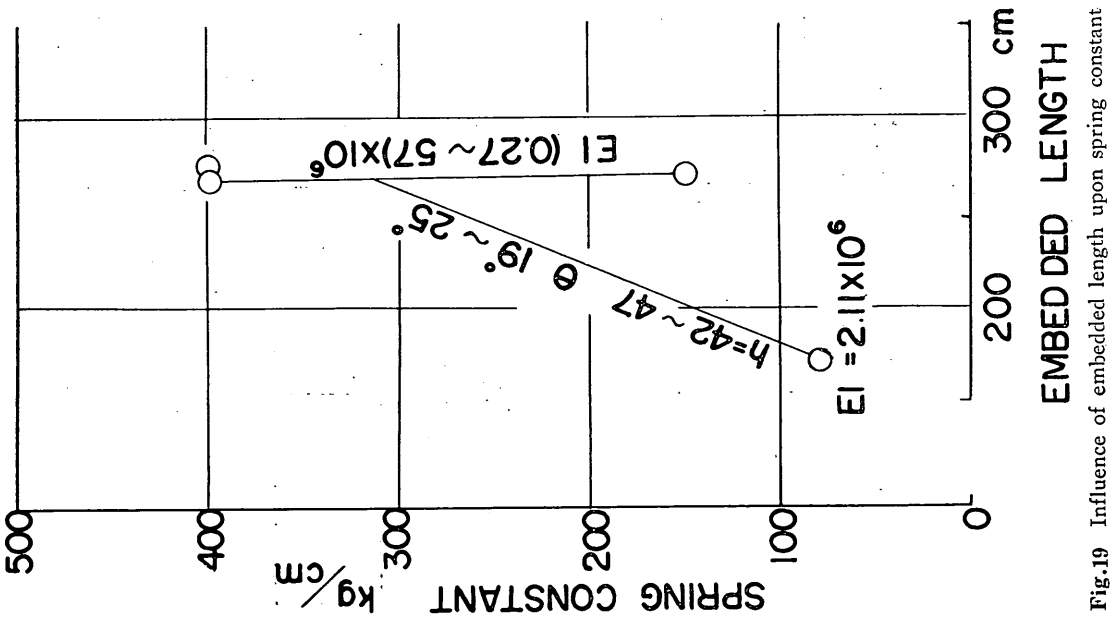

Fig.19 Influence of embedded length upon spring constant

In the graphs presented above there is some range of figures representing the pile conditions, but this reason is due to unavoidably erratic installation of the model coupled piles.

As a result, in the effect of several piles condition upon the spring constants of the coupled piles, the following items can be concluded.

1) As the angle of batter increases, the horizontal resistance expressed by a spring constant of the coupled piles increases.
2) The effect of flexural rigidity upon the horizontal resistance is indistinct.
3) The effect of height of load application upon the horizontal resistance can not be discerned.
4) The effect of the embedded length upon the horizontal resistance is obvious neither.

The above-mentioned conclusions can be readily deduced from the fact that a horizontal force acting at the intersection of the coupled piles is counteracted mostly by the axial resistance, and, if they are examined by the equation for a spring constant pertaining to the coupled piles which can be derived from Eq.6 under an assumption that the angle of batter, the axial and the lateral spring constants of the two piles are all the same.

In this equation, ω was much larger than μ by second order in this case. If θ increases, the first term becomes dominant to K while the second term diminishes.

The effect of flexural rigidity on K can be also deduced from the fact that the peripheral length affecting ω hardly increases while ω becomes larger accordingly as the flexural rigidity increases. This variation scarcely affects K as a whole.

The embedded length has no relationship with μ whereas its enlargement induces

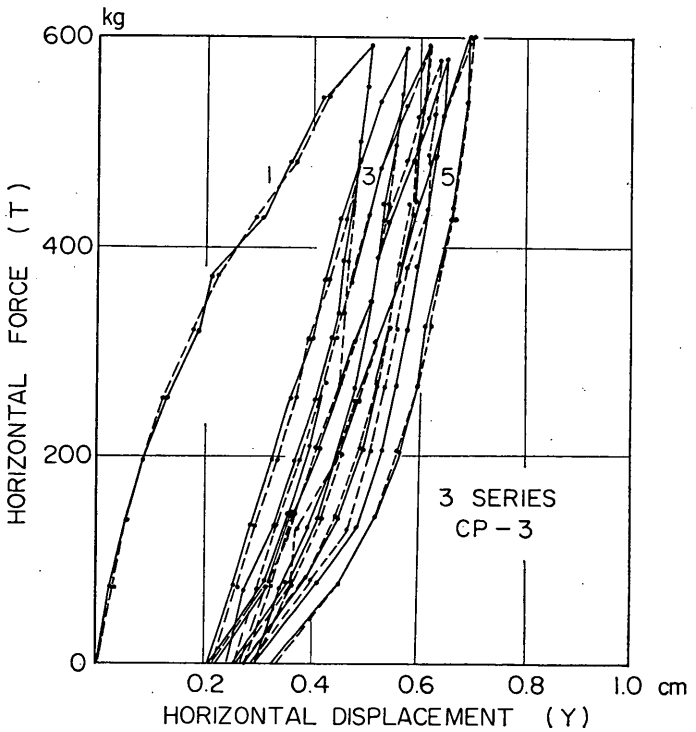

Fig.20 Result cf repeatedly loading test

an increasing in ω. Therefore, it will enlarge K but indistinctly.

The result that the height of load application has scarcely any effect on the spring constant can be also explained from the equation in such a manner as μ decreases and ω hardly changes with an increment in the height of load application.

Fig. 20 illustrates the horizontal behavior of the coupled piles subjected to repeatedly loading. This is only a demonstration expressing the fact that the residual displacement is obviously accumulated with the number of repetition. This phenomenon means that a repeated load acting at the coupled piles corresponds to an apparantly increasing external force likewise as in the case of a single pile.

In Fig. 21, vertical displacements at the intersection of the coupled piles in 6th series are plotted against the horizontal force. From this graph it seems that there is

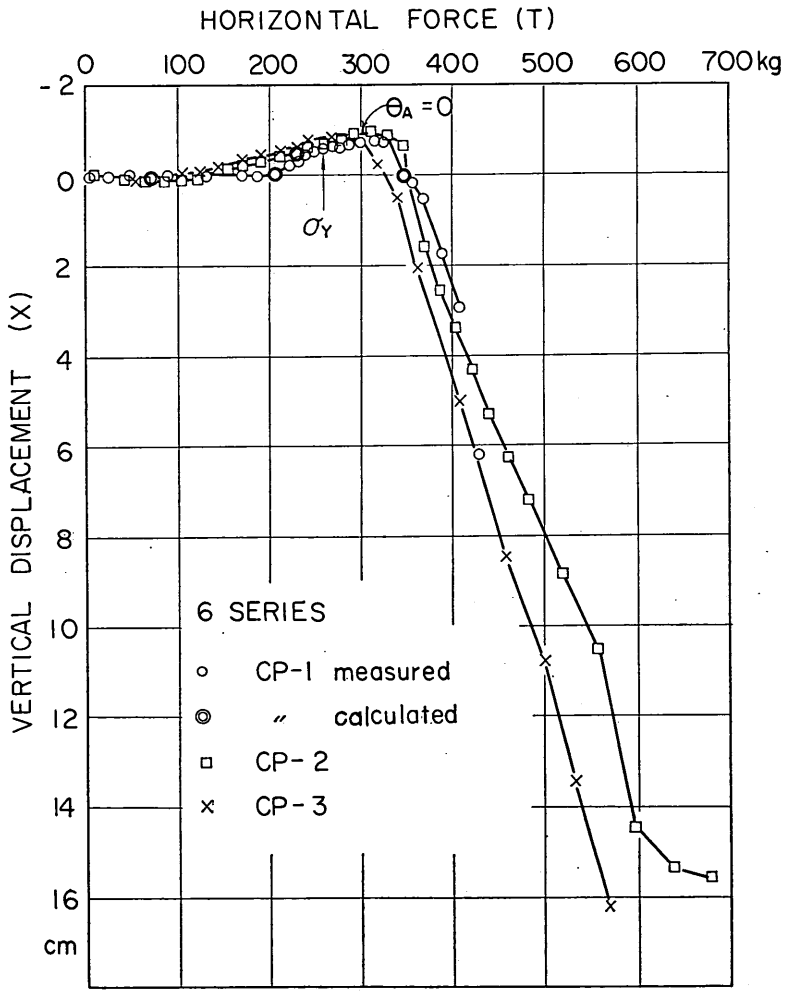

Fig.21 Horizontal force and vertical displacement curves

little difference between the hinged and fixed intersection, and either curve shows a little rise-up and an abrupt descent at some horizontal forces. σ_y indicates a point where the fiber stress becomes up to yield and at the peak of these curves the inclination of the upper part of the out-batter pile becomes zero ($\theta_1=0$). Double circles indicate the results estimated by the new method of computation.

While any vertical displacement hardly occures during the early stage of loading until the horizontal force attaines some magnitude which will be corresponded to the maximum pulling resistance as described later, the piles after the peak are remarkably bent over.

It was disclosed by an excavation of the test ground that the in-batter pile was bent with a slow curvature and leant over the out-batter pile which was bent sharply.

Photo.1 Bending of coupled piles after loading (hinged-head)

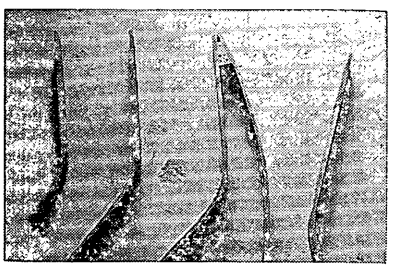

Photo.2 Bending of coupled piles after loading (fixed-head)

This disclosure means that the bending yield occured at one point in the out-batter pile while it occured progressively from a point to another in the in-batter pile when it was pulled up.

Photo.1 shows the embedded portion of the model hinged-head coupled piles after extremely heavily loading, and indicates the fact that the in-batter pile was bent smoothly but the out-batter pile was bent sharply. This sharply broken point corresponds to the maximum bending in the pile. Photo.2 shows the fixed-head coupled piles which were dug out after loading. A small crack was also seen near the intersection of the coupled piles.

In Fig.22 and Fig.23, the typical moment diagrams of two coupled piles are respectively illustrated which are obtained by strain gauges measurement. Though the moment diagrams corresponding to the piles remarkably bent over in 6th series could not be expressed because the conversion factor from strain to moment could not be determined, the diagram represented in Fig.23(b) gives as much bending moment as the whole cross-section of the piles became plastic at the maximum.

In all tests but the coupled piles with inactive strain gauges, the moment diagrams were similarly completed and in all cases they were found out to have the same shape as that characteristic to a single pile. In these diagrams, little difference in bending moment between the in-batter and out-batter pile can not be discerned, and

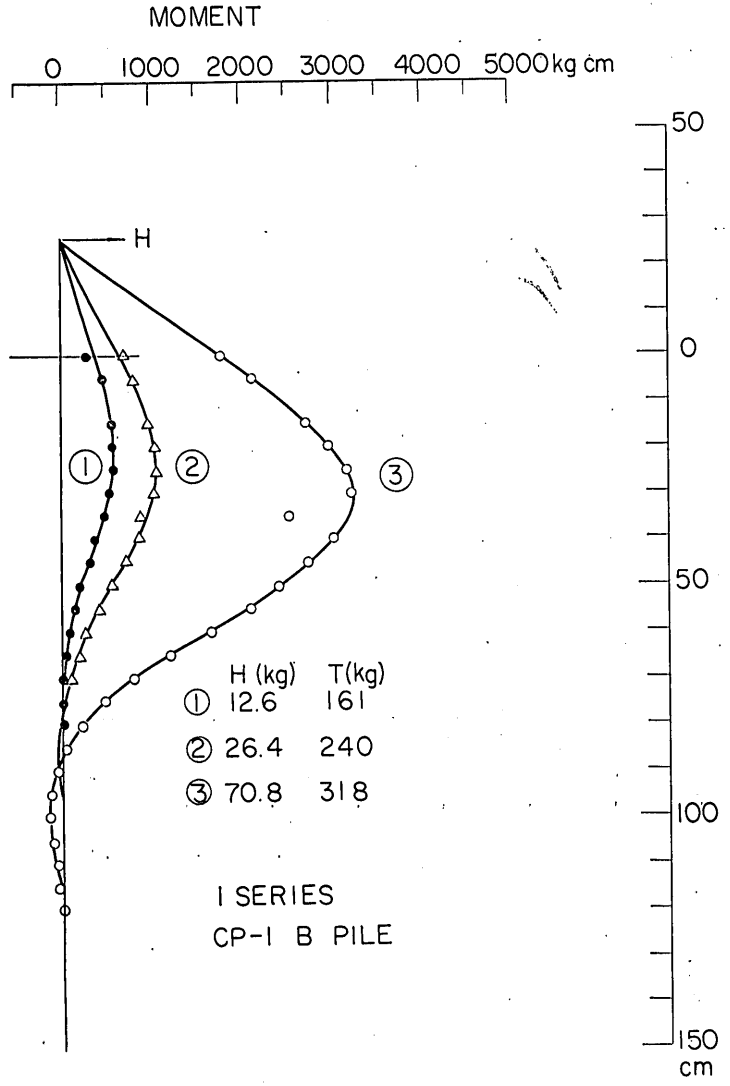

Fig.22(b) Moment diagram (B-pile, CP-1, 1st series)

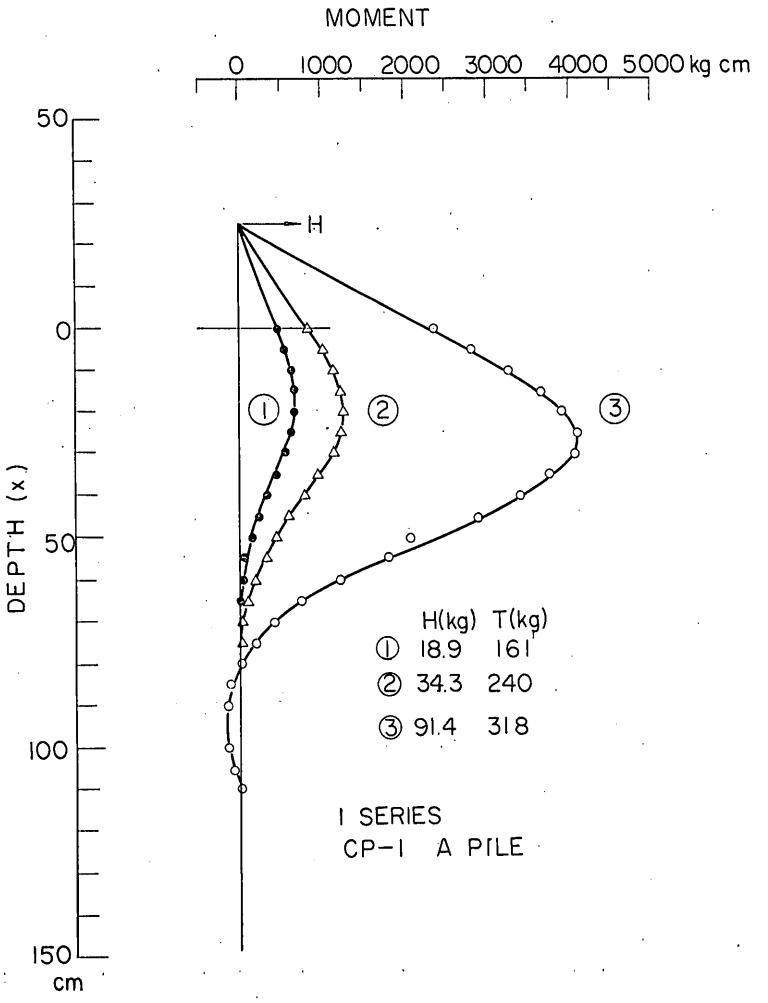

Fig.22(a) Moment diagram (A-pile, CP-1, 1st series)

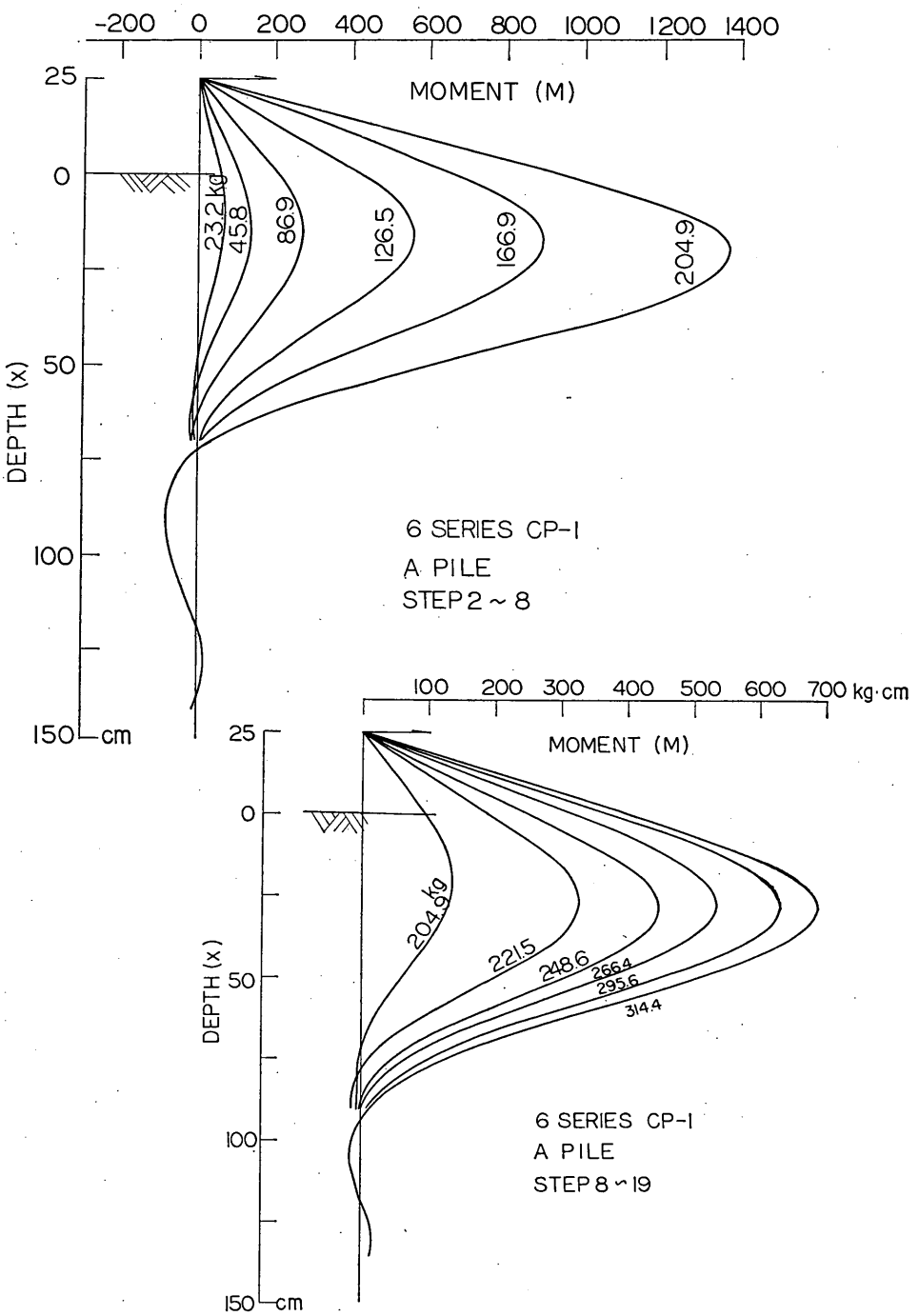

Fig.23(a) Moment diagram (A-pile, CP-1, 6th series)

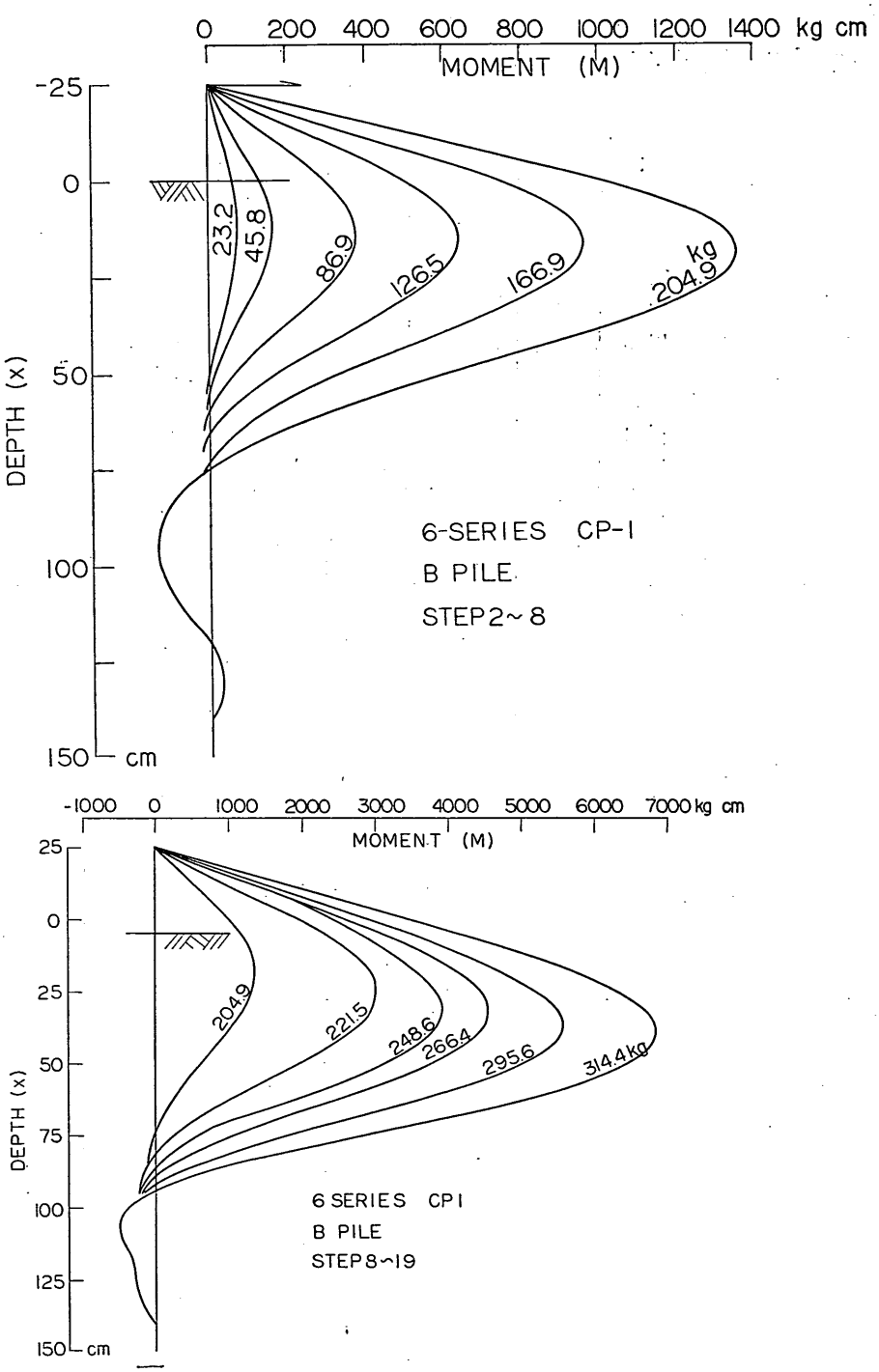

Fig.23(b) . Moment diagram (B-pile, CP-1, 6th series)

so, on the basis of these diagrams, the variations of the maximum bending moment and of the depth to the first zero point of moment diagrams with the lateral force

are plotted in Fig.24 to Fig.27.

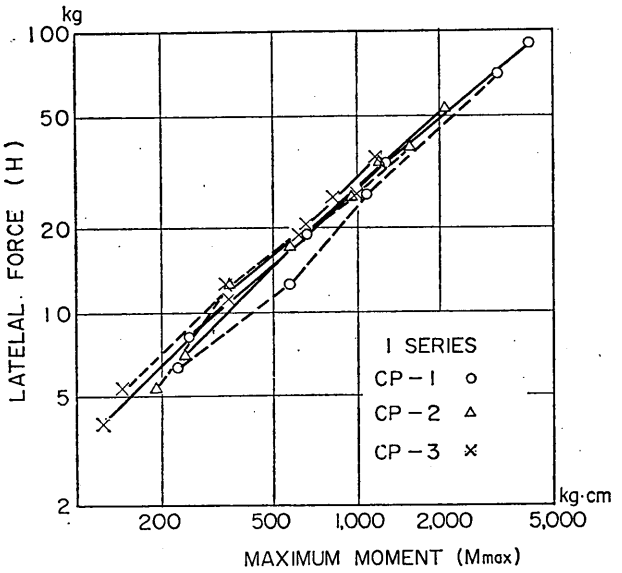

Fig.24 Maximum moment (1st series)

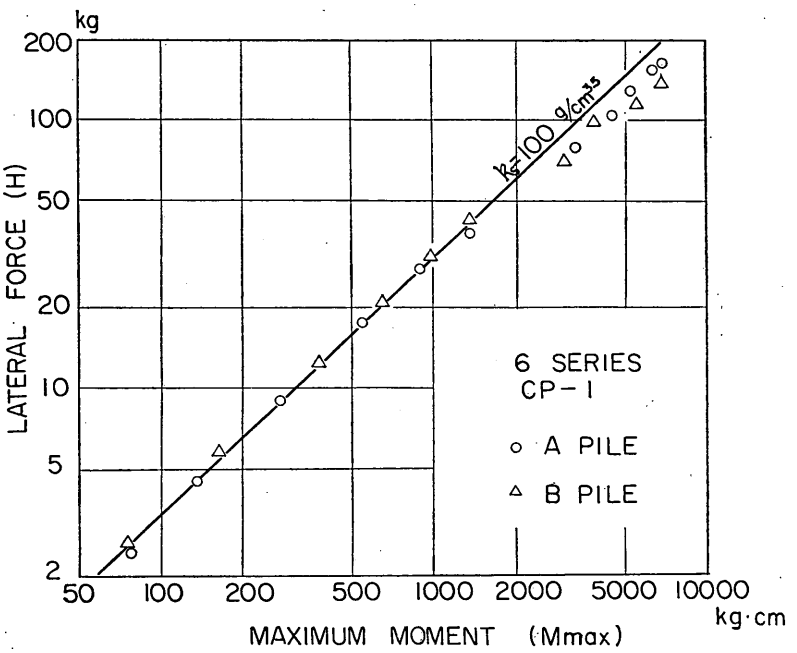

Fig.25 Maximum moment (hinged-head, 6th series)

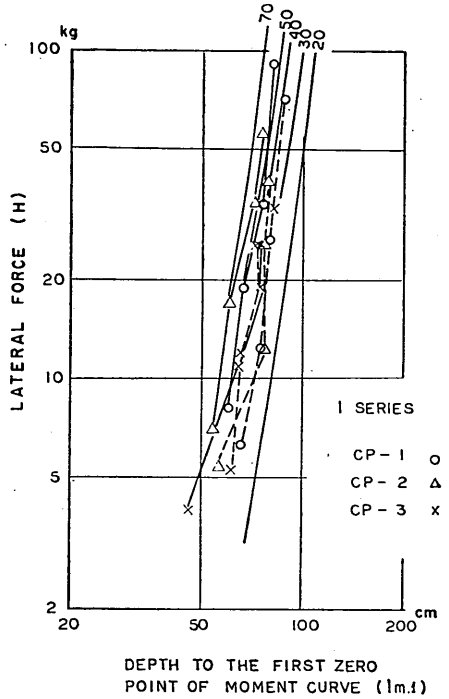

Fig.26 The depth of the first zero point of moment curve (1st series)

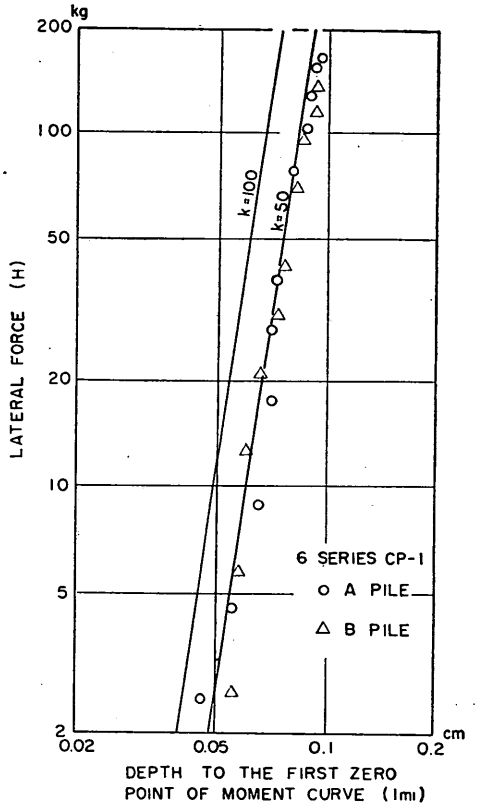

Fig.27 The depth of the first zero point of moment curve (6th series)

The lateral forces at the top of the piles are calculated from the first differentiation of moment diagrams. The solid line or A-pile corresponds to the out-batter pile and the dotted line or B-pile corresponds to the in-batter pile.

In these graphs the estimation curves fitting to the measured values as near as possibly are added which can be built on the basis of the Kubo,s method. It can be seen that the measured values are scattered in parallel with the estimation curve, and in consequence the lateral behavior of each member of coupled piles will be similar to that of a single pile.

In the Kubo's method, such a relationship between deflection y of a pile and soil reaction p as

$$p=k_s x y^{0.5} \tag{10}$$

is assumed to exist as the results of laboratory tests on a single pile subjected to a lateral force. In this expression k_s is called a coefficient of soil reaction and only dependent on soil properties and the width of a pile.

The estimation curves which are shown in the above-mentioned graphs can be built under a given k_s and each pile condition. The magnitude of k_s means the

degree of lateral resistance of the ground relative to a pile stiffness.

Therefore, k_s pertaining to the estimation curves fitting to the measured values as near as possibly indicates the degree of lateral resistance of the measured pile. k_s should have been coincident in any kind of measured values for the same pile, but there seems to be a little dispersion in these results because of the error in graphical calculation with moment diagrams or a slight difference from a single pile.

In Fig. 28, the relation between the maximum moment and the lateral force with respect to fixed-head coupled piles is represented, and the estimation curves having $k_s=100\text{g/cm}^{3.5}$ in both a free-head and a fixed-head pile are written down.

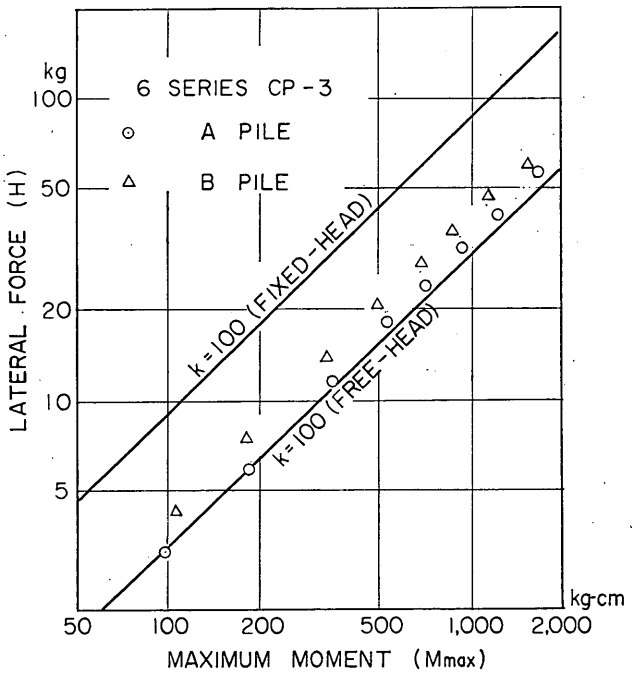

Fig.28 Maximun moment (fixed-head,6th series)

The way to obtain k_s directly is to plot p/x against y at a depth x on a double logarithmic scale as shown in Fig. 29 to Fig. 30(a) and(b), to draw a curve in average through the plotted values and to pick the ordinate on $y=1$cm. In these graphs the measured values are never completely drawn up on one line, but a representative line as an average has a slope of one in two and is approached by the measured values. This fact means also that the lateral behavior of each pile is similar to that of a single pile.

Fig. 31 and Fig. 32 show the relation between a lateral force and displacement in the so far mentioned cases, with addition of the estimation curves. In 6th series the lateral displacement of the two batter piles changes place at some lateral force, but in lst series this phenomenon can not be seen. In these graphs the measured values are plotted along the estimation curves corresponding to the respective k_s. This result also indicates the fact that the member of the coupled piles behaves laterally

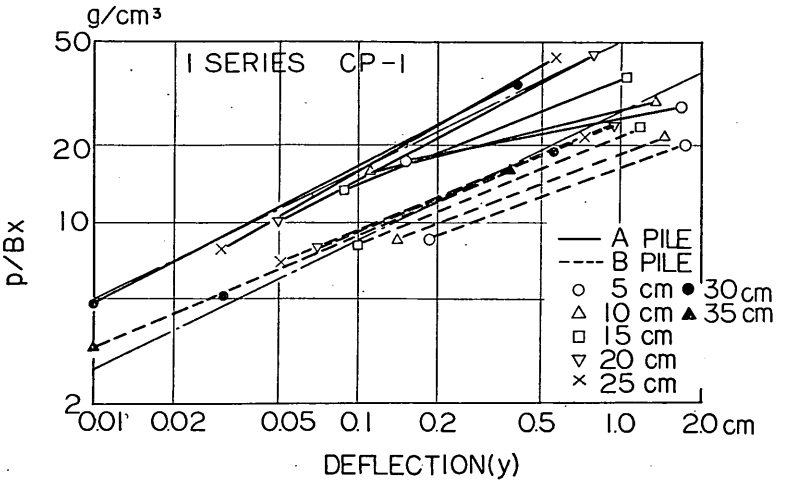

Fig.29 $P/Bx \sim y$ relationship (lst series)

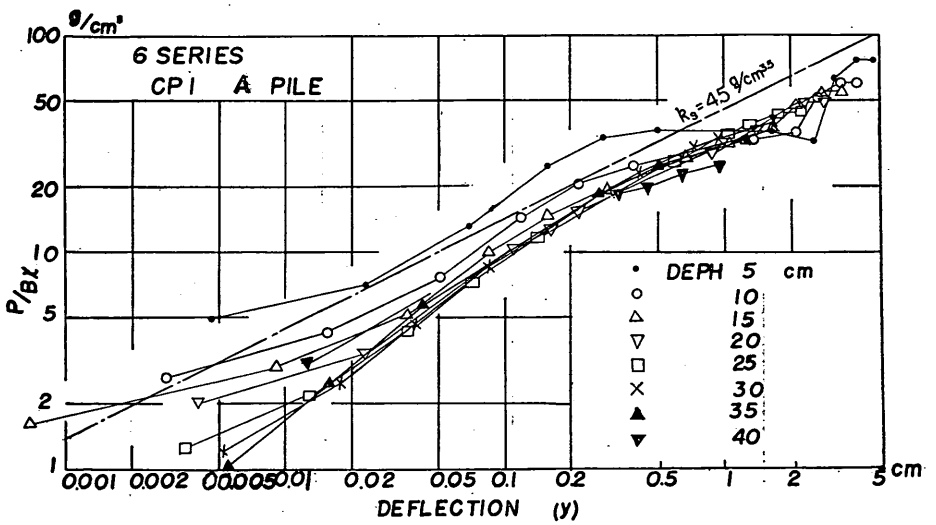

Fig.30(a) $P/Bx \sim y$ relationship (A-pile, 6th series)

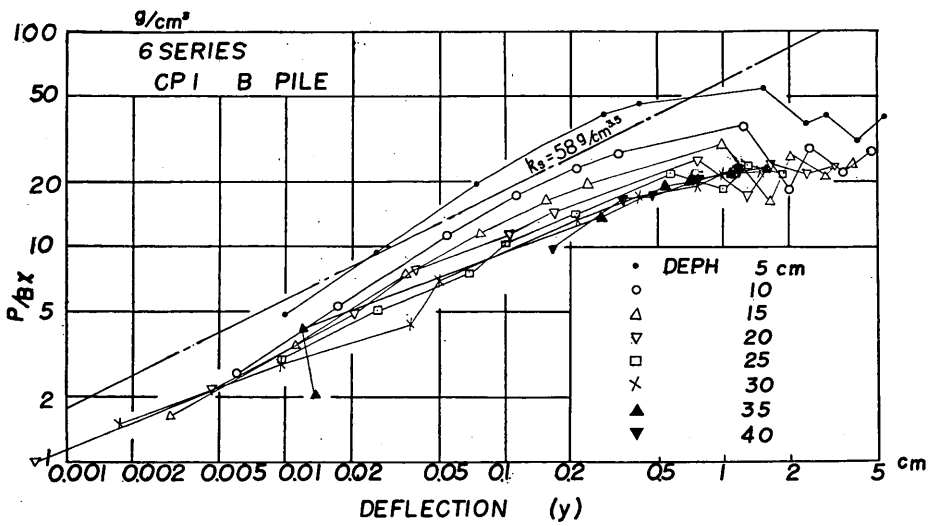

Fig.30(b) $P/Bx \sim y$ relationship (B-pile, 6th series)

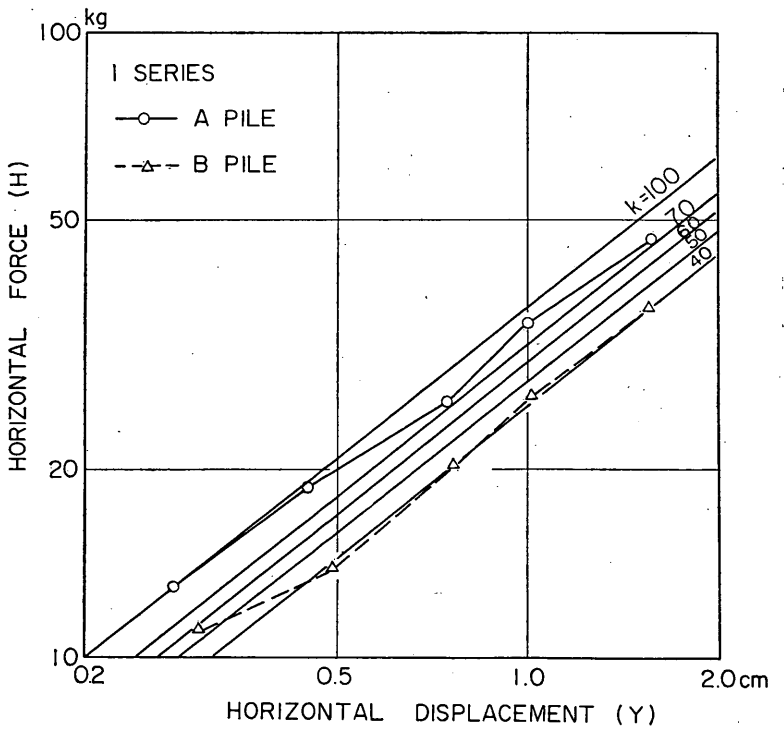

Fig.31 Lateral force and displacement curve (lst series)

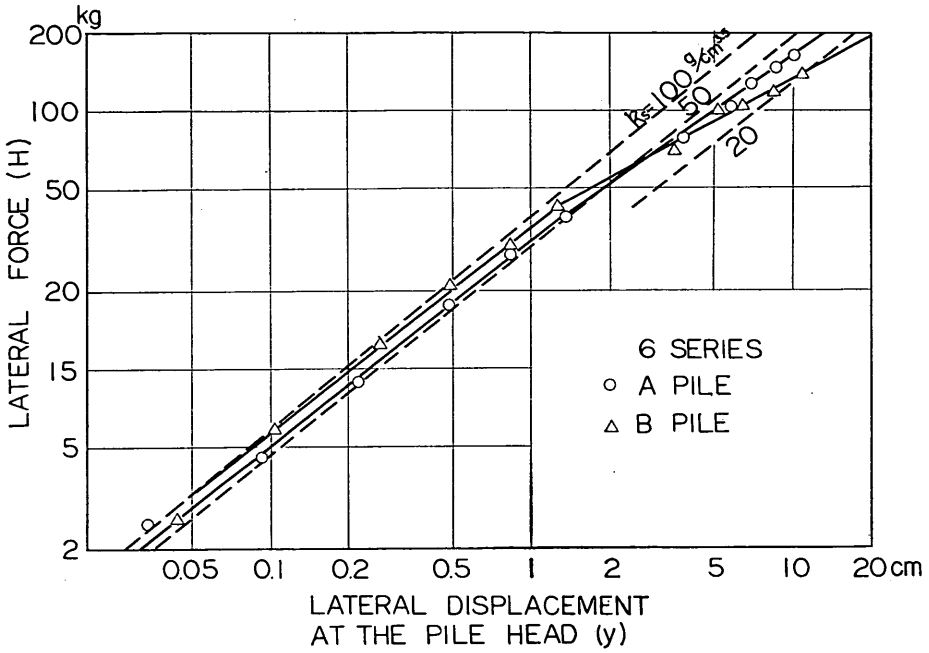

Fig.32 Lateral force and displacement curve (6th series)

likewise as a single pile.

As a summery concerning to the lateral behavior of all the piles as described so far, k_s which represents the measured values in every graph as much fittingly as possible is tabulated through all the tests in Tab.4.

Tab. 4 Evaluation of k_s values (kg/cm$^{3.5}$)

SERIES	PILE NUMBER	FROM $P/Bx \sim y$ CUYVE		FROM $S \sim y$ CURVE		FROM S-l_{m1} CURVE	
		A-PILE	B-PILE	A-PILE	B-PILE	A-PILE	A-PILE
SR-1	CP-1	38	21	80	40	50	32
	〃 2	60	27	110	53	60	40
	〃 3	70	63	120	160	40	40
	〃 4	—	—	—	—	—	—
SR-2	CP-1	64	52	—	—	60	40
	〃 2	41	51	—	—	65	45
	〃 3	—	—	—	—	—	—
	〃 4	—	—	—	—	—	—
SR-3	CP-1	—	—	—	—	—	—
	〃 2	42	33	43	50	10	10
	〃 3	41	27	40	31	45	24
SR-4	CP-1	—	—	—	—	—	—
	〃 2	33	28	—	—	26	20
	〃 3	23	38	50	30	40	32
SR-5	CP-1	27	34	25	40	38	40
	〃 2	34	20	40	30	48	55
	〃 3	175	80	60	30	100	70
SR-6	CP-1	45	58	60	80	50	50
	〃 2	46	55	60	60	35	40
	〃 3	43	42	—	—	34	30

The conclusions deduced from the table are as follows; 1) There is to some extent dispersion of k_s in the respective graphs in spite of the same pile, but this seems to be caused by the inevitable errors when picking the measured values on graphical calculation in addition to the measuring errors. 2) k_s of the two piles, which represents the degree of compactness of the test ground, shows an opposite aspect in magnitude between lst to 5th series and 6th series. This reason can be considered due to a different degree of compaction.

In the past, the fact that k_s increased as the angle of batter measured from the load direction increased was disclosed. Judging from this feature, it seems that the soil deposited between the two piles in lst to 5th series was not so much densely compacted as the soil deposited outside.

But, anyway, it is rather difficult to point out a difference in magnitude as to the lateral behavior between the two piles.

3) Though there are still remained undetected effects on the lateral behavior of each pile, it can be considered to be similar to that of a single pile as far as the results of this test are conscerned.

Thus far, the lateral behaivor of each pile has been scrutinized, and the next problem is its axial behavior. It had been expected to know the axial force of each pile at one-gauge measurement, but the axial strain was so much less than the bending strain as included into the errors of measurement. Any illustration as to the measuring axial strain is not presented, but in rough appraisal the rate of axial strain to bending strain at the pile surface is one to one hundred.

For the above reason, the axial strain was indirectly determined from the equations

$$\left.\begin{aligned} N_1&=\frac{T\cos\theta-H_1\cos2\theta-H_2}{\sin2\theta}\\ N_2&=\frac{T\cos\theta-H_2\cos2\theta-H_1}{\sin2\theta}\end{aligned}\right\}\qquad(11)$$

which can be obtained from the equilibrium of forces at the intersection to the direction of the two pile shafts. In these equations, the two lateral forces can be calculated by first differentiation of the moment diagram as equivalent to a shearing force at the top.

Fig.33 and Fig.34 show typical results of the computated axial forces against the horizontal applied force at the intersection of the coupled piles together with the relation regarding the lateral forces. In Fig.34 double circle marks represent the values obtained by the new method of computation. As far as these graphs are concerned, the axial force is considerably larger than the lateral one, but, as stated before, the maximum stress producted by the lateral force is remarkably higher than that producted by the axial force. An attribution of the lateral force to the horizontal resistance of the coupled piles could be considered in its horizontal component expressed with the use of percentage of share.

Fig.35 to Fig.37 show the relations between the axial force and displacement of the tops of members of the coupled piles (a downward load and settlement in the case of the out-batter pile or a pull and rise in the case of the in-batter pile), where the displacement was measured by dial gauges. In Fig.37, the solid lines represent the relationship obtained from the measurement on coupled piles, and the dotted lines represent the results obtained from the loading test and the pulling test on a single batter pile for the purpose of comparision with both the axial bearing mechanism.

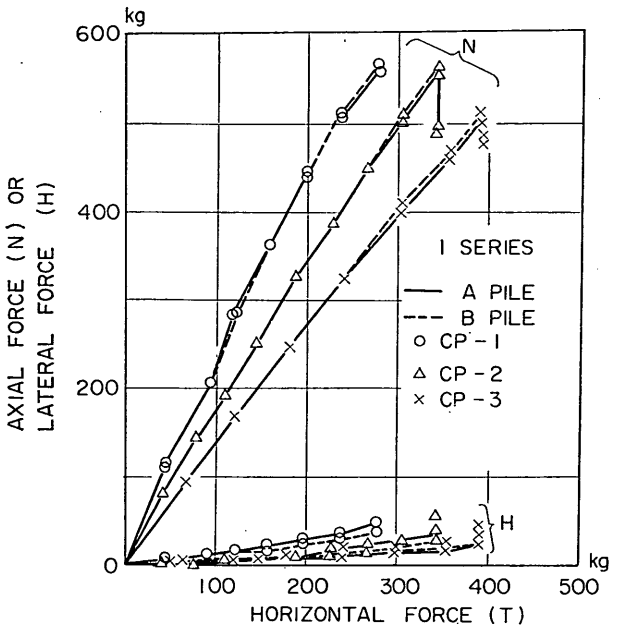

Fig.33 Axial and lateral force against horizontal force (lst series)

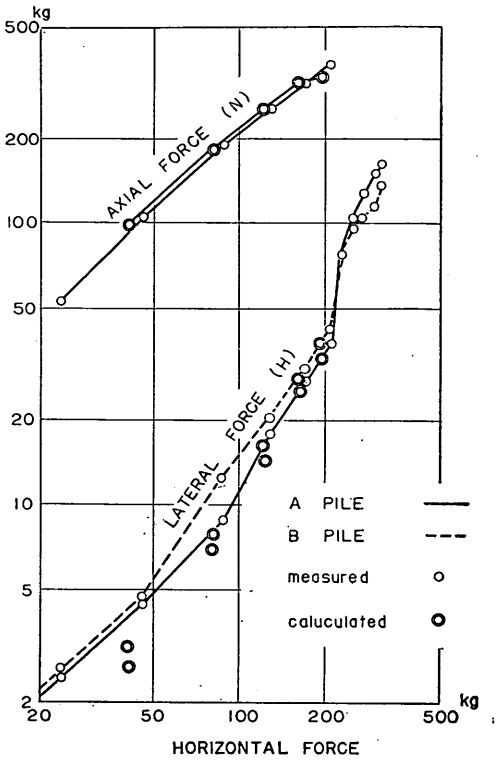

Fig.34 Axial and lateral force against horizontal force (6th series)

A definite difference can be seen between the results in lst to 5th series and those in 6th series; in the former, little difference exists in the absolute measured values between the two piles, but, in the other hand, the latter result where the piles were loaded highly shows a definite difference between the two piles.

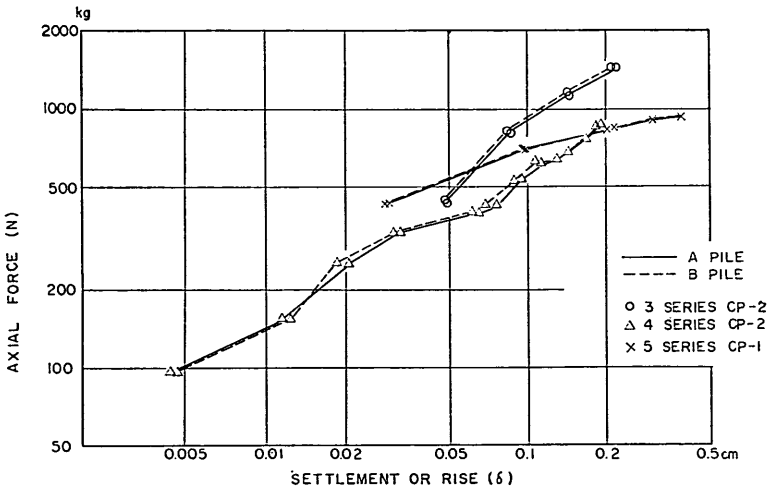

Fig.35 Axial force and displacement curves (3rd to 5th series)

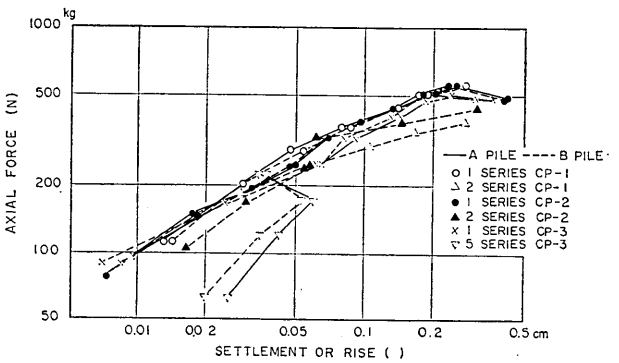

Fig.36 Axial force and displacement curves (1st and 2nd series)

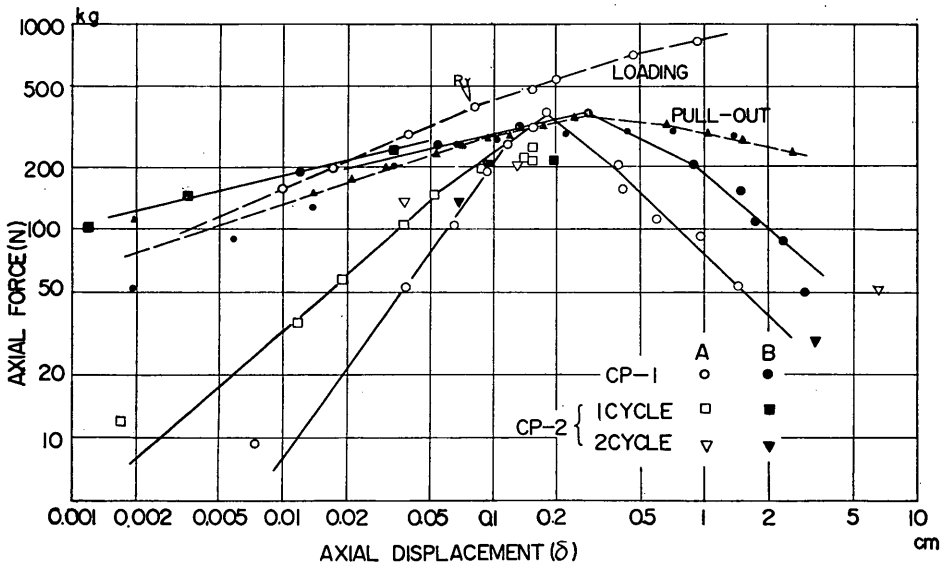

Fig.37 Axial force and displacement curves (6th series)

These curves appear in straight lines on a double logarithmic scale except the existance of a peak in 6th series. This peak seems to indicate the maximum pulling resistance of the in-batter pile (R_m=320kg), which is nearly the same as the value measured from the pulling test on a single batter pile. The yield valve R_y of a single batter pile downward seems to be about 600kg from an indistinct break point of the diagram. But the bearing resistance before yield is much higher in a single pile than in the out-batter pile. This may be caused by the different soil condition in addition to the influence by deflection of the out-batter pile.

The horizontal force corresponding to this pulling resistance is about 200kg as indicated in Fig.34, Consequently, the previous description that the horizontal applied force at the moment when the vertical displacement of the intersection of the coupled piles started to rise up corresponded to when the pulling resistance of the in-batter pile became the maximum will be proved out.

Fig.37 shows additionally the result that the out-batter pile also indicates the peak value at almost the same time as when the in-batter pile does, in contradiction

to the fact that the downward resistance of a single pile increases or, at least, becomes constant as it goes down.

This phenomenon can be interpreted as the result of a transference with a great part of horizontal force resisted by the axial bearing capacity of the out-batter pile to its bending moment immediately after the in-batter pile attaines the maximum pulling resistance.

In 6th series, the behavior of the two piles are considerably different from those of the previous series even though the pile conditions are all the same, but it is not easy to say which is the true phenomenon because of the existance of the errors induced on both the measurement and the calculation process. However, it is obvious that it will be misleading to estimate the behavior of the coupled piles exceeding the

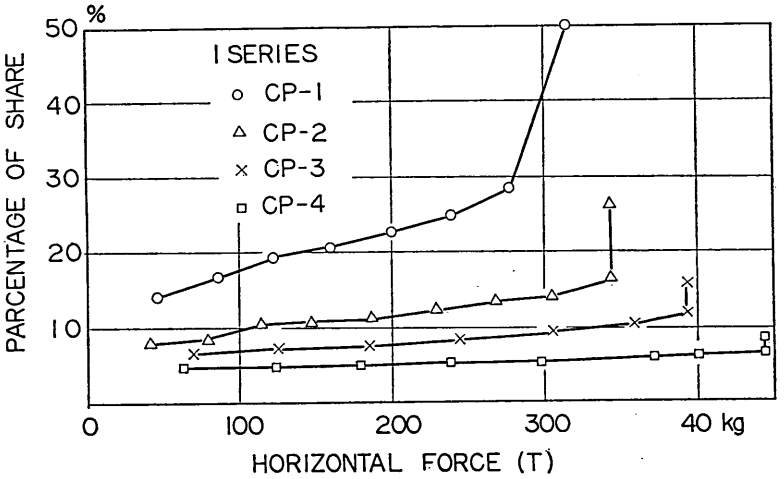

Fig. 38 percentage of share influenced by angle of batter (lst series) (fromK. Kubo)

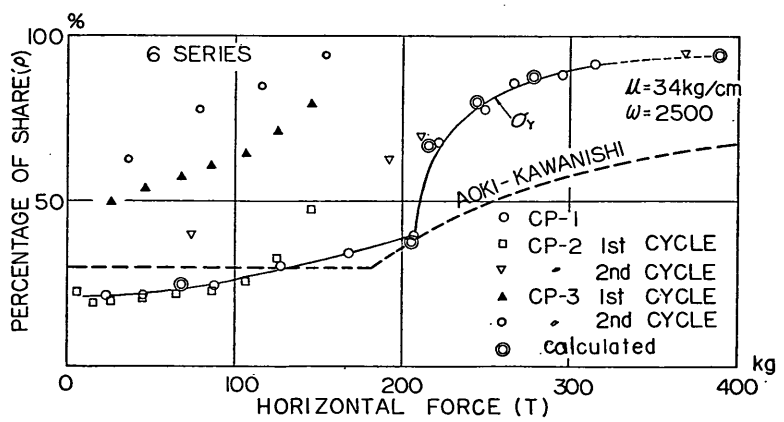

Fig.39 percentage of share (6th series)

maximum pulling resistance of the in-batter pile from the data as to load tests on a single vertical pile.

As stated before, the percentage of share can be used for representation of the attribution to the horizontal resistance of the coupled piles by bending moment. Fig. 38 illustrates that the percentage against the horizontal force in lst series which is

published in Kubo's thesis. Fig.39 is the same kind of graph in 6th series.

In both graphs it is obvious that the percentage at early stage of loading is relatively small, but at some horizontal force it ascends abruptly. In 6th series, this boundary force corresponds to the maximum pulling resistance of the in-batter pile, but in lst series other data to go upon could not be found out except the results that vague peaks could be recognized in the relation between the axial force and displacement as shown in Fig.35.

Fig.38 expresses also the result that the increment in the angle of batter diminishes the percentage of share and enlarges the boundary horizontal force.

Fig.39 shows that the percentage of shear after the maximum pulling resistance becomes closer to almost one hundred percent in the case of hinged-head coupled piles. But the percentage in the fixed-head coupled piles is comparatively higher even at early stage of loading.

Double circles mean the values calculated by the new method of computation, and σ_y means the point where the fiber stress became up to yield. Yield in fiber stress succeeds attainement of the maximum pulling resistance.

In this graph the dotted line is built on the basis of the method of computation proposed by Aoki or Kawanishi. This estimation method gives a fairly good answer at early stage of loading if the axial and lateral spring constants are adequately chosen.

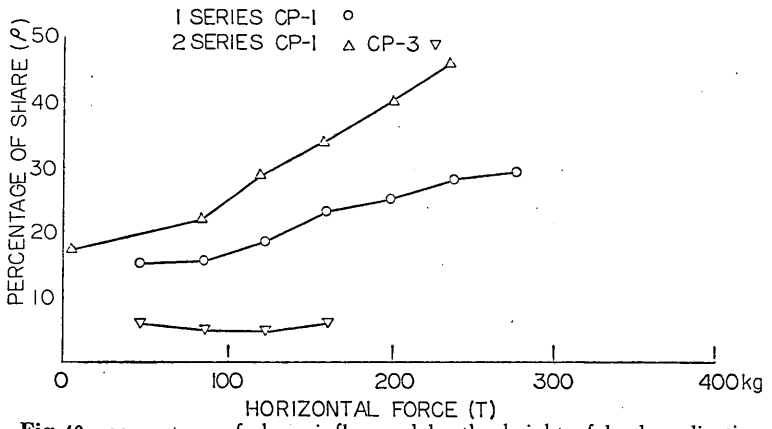

Fig.40 percentage of share influenced by the height of load application

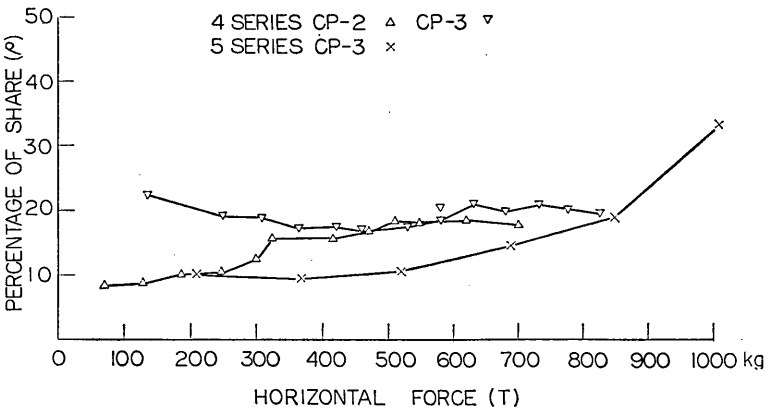

Fig.41 percentage of share influenced by flexural rigidity

The percentage of shares against the horizontal force in other series than lst and 6th series are illustrated in Fig.40 and Fig.41 to the end that the influence of piles condition except the angle of batter upon the percentage is investigated.

Fig.40 where the influence of height of load spplication is compared shows that the coupled piles with larger height of load application have a smaller percentage. The graph concerning to the influence by flexural rigidity on that percentage shows that the coupled piles with larger flexural rigidity has a larger percentage as shown in Fig.41. The investigation on the influence of embedded length upon the percentage of share could not carried out on account of insufficient data.

These characters might be explained coincidentally with the use of the expression given in Eq.5. If the angle of batter increases the numerator of the equation will obviously decrease, and so it results in a decrease in the percentage. An increase in flexural rigidity induces an increase in the axial spring constant, which is followed by an considerable increase in the numerator comparatively to an increase in the denomenater, and in consequence the percentage is increased. As the lateral spring constant decreases with an increase in the height of load application, the numerator decreases remarkably with comparision to an decrease in the denomenater, which results in an decrease in the percentage.

Thus, the expression is rather useful for qualitative consideration on these influence of pile conditions.

The fact that the percentage of share is much more in the fixed-head than the hinged-head coupled piles is considered to be caused by the reason that a larger shearing force would be induced to resist a moment at the fixed head.

As shown in Fig.39. the estimation by the new method of computation represents the real behavior of the coupled piles infallibly, but, the axial and lateral load-displacement relationships used for the computation are based on the measured values in the model tests. Therefore, if the same relationships obtained from the load tests on a single pile is used, the results will differ to some extent. However, even though the computation is based on the measurement of the same test, the fact that the horizontal behavior of the coupled piles estimated by the new method coincides with the observed phenomena gives the prospect that, if a suitable revision is added to the results obtained from a single pile, the accurate lateral behavior of coupled piles can be estimated.

In addition to this benefit, this method has an advantage of possibility to investigation on the mutural influence of the axial and lateral behavior of members in coupled piles, because a difference between the results obtained from a single pile and the real phenomena of coupled piles will represent the mutural influence in itself.

For this reason, the predicted procedure for the revision will be described in the next chapter.

5 Procedure of Revision for the New Method

Several different points from the behavior of a single pile have been found out as members of coupled piles as seen, for example, in Fig.37. In fact, these different points seem to be of little importance in practical design, but if the considerably accurate estimate is demanded for the lateral resistance of coupled piles, it may be necessary to revise the load-displacement curves correspondingly to the coupled piles

conditions.

The items to be revised are as follows; an influence of bearing capacity of a pile due to its lateral deflection, pile spacing, angle of batter and embedded length with respect to the axial behavior, and angle of batter and pile spacing with respect to the lateral behavior. The revisary procedure with respect to the axial behavior can not be mentioned nothing yet, but it should be borne in mind that such phenomena will happen as the skin friction in the out-batter pile is reduced along the side apart from the attached soil while it increases along the opposite side as the pile is deflected more and more and its deflection accelerates the settlement of the top, and as the skin friction in the in-batter pile decreases along both sides as it is deflected while its deflection diminishes the rise.

If the spacing of the two piles gets narrower, these piles affect each other on their axial behavior through the interposing soil. This seems to be similar to the phenomena occuring between a test pile and the anchor piles in axially loading tests. At any event any study on the mutural influence of piles closely driven, one going down and another rising, on their axial behavior can not be found out.

The revision with the angle of batter can be done by modifying the embedded length penetrating in the soil layers. Therefore, a batter pile has a substantially different ultimate axial resistance from that of a vertical pile, but the fundamental character in such a mathematical expression as, for example, in Eq.12 will not change.

Concerning to the revisary procedure with the angle of batter in a lateral movement at the top, a relation between the angle of batter and the coefficient of soil reaction can be used which had been already published by Dr. Kubo in the sixth International Conference on Soil Mechanics and Foundation Engineering. In that paper, the coefficient of soil reaction increases as the angle of batter measured from the force direction increases.

In addition to this revision, consideration should be taken into regarding an influence of pile spacing on a lateral movement. In this case, pile spacing should be represented by a ratio of its distance to the pile diameter. This revisary procedure for a coefficient of soil reaction will be able to be partly refered to the incomplete results obtained from the laboratory tests. An outline of the test is already described in Chap.3. Accordingly to the description it is obvious that a coefficient of soil reaction decreases as the distance between each pile gets narrower than a certain value. If the unsuported height of coupled piles is so small that some influence of pile spacing is feared to occure, the revision must be carried out by using this kind of result. In this result, only the effect of the back pile on the fore pile was investigated, and the contrary case should have been added.

A supperposition with the above-mentioned revisals makes surely approach to the real phenomena as members of coupled piles with the original characters pertaining to a single pile. But, as stated hitherto, most of the revisary procedures are still in question so that it is to the utmost to estimate the approximate movement of coupled piles on the basis of the original data.

6 Neumerical Analysis on the Test Results

The ultimate bearing capacity of the out-batter pile can be estimated as a single pile from the Meyerhof's formula, which is based on the standard penetration values

measured in the driven site, as follows;

$$R_u=40NA_p+\frac{\bar{N}A_s}{5} \tag{12}$$

where R_u is the ultimate bearing capacity of a pile, N is the standard penetration value at the tip, $\bar{N}$ is average N value along the embedment, A_p is the cross-sectional area and A_s is the peripheral area of a pile, expressed in ton and meter as unit. The maximum pulling resistance can be obtained from the second term of the equation.

Considering the test results of CP-1 in 6th series only, the following informations are given by the soil exploration and the pile dimensions;

$N=8.0$

$A_p=0.00084\text{m}^2$

$A_s=0.236\text{m}^2$

$\bar{N}=5$

where the values were induced from the blow numbers in dynamic cone penetrometer as shown in Fig.10; that is, a ratio of 1 to 2.9 was obtained from a comparision with the N value and the dynamic cone penetration value at the depth of 100cm in the test ground, a conversion could be applied to know the N value at other depth.

As a substitution into Eq.12 with these figures, the ultimate bearing capacity R_u becomes 500kg and the maximum pulling resistance R_m becomes 270kg. On the other hand, the yield value R_y of the same kind of single batter pile as the out-batter pile could be determined as about 400kg from a first slight break of the load-settlement curve as indicated in Fig.37, and the maximum pulling resistance of a single batter pile in the in-batter direction was about 320kg. As R_u is said to have a value exceeding R_y by 50%, the estimated R_u and R_m are much higher than the measured values. This seems to be caused by an additional skin friction due to the coating materials on the sides of the testing piles, unjustifiable application of the Meyerhof's formula upon the model batter pile, and so on. Furthermore, the maximum pulling resistance measured from the in-batter pile of the coupled piles was nearly thre same as R_m of a single pile, but R_u of the out-batter pile could not be determined as explained in Chap.3. Now, for the purpose of an execution of numerical analysis of the coupled pile, let us assume that the single batter pile has 600kg ($=400\text{kg}\times1.5$) as R_u and 320kg as R_m.

With the use of the value, the axial spring constant can be estimated by Eq.22 which is presented in Appendix, as

$$\omega=0.4\times0.60=0.24\ \text{t/cm}$$

On the other hand, it can be estimated also by using Eq.23, which is presented in Appendix, with substitutionf or $A_p=8.4\text{cm}^2$, $E=2.1\times10^6\text{kg/cm}^2$, $\lambda=25.4\text{cm}$, $\nu=8/15$ and $l=170\text{cm}$, as

$$\omega=\frac{8.4\times2.1\times10^6}{25.4+170\times8/15}=0.152\times10^3\text{t/cm}$$

These two results differ by three powers. Average axial spring constants measured by the test are 2.55t/cm downward and 20t/cm upward, which corresponds to a secant modulus of a slope intersecting through a point of one-half the maximum in the load-displacement diagrams.

For the purpose of comparision with spring constants pertaining to the actually

used piles in the fields, the collected data are illustrated in Fig.60, which is presented together with the ground conditions, in Appendix. In this case, they correspond to a secant modulus of a slope passing through a point at the settlememt of 10mm. These values are located within a range of 100～200t/cm on an average.

With respect to the lateral spring constant of the test piles, the Chang's formulae (Eq. 24 to Eq. 26) are the most applicable to its estimation on the basis of the results of soil exploration: as the N value is found out to be 4, the coefficient of horizontal subgrade reaction k_h turns out to be 0.8kg/cm^3 from such a relation between the N value and k_h as indicated by Yokoyama. The modulus of elasticity of soil E_s can be obtained by multiplying with the width of the pile of 7cm, as 5.6kg/cm^2. Then relative stiffness β (see symbols) becomes 0.0288cm^{-1}, with which the substitution into Eq.24 results in

$$\mu=\frac{5.6}{2\times 0.0288}=0.097\text{t/cm}$$

On the other hand, the lateral spring constant at 10mm as measured by the test becomes $\mu=0.034$t/cm, which is smaller than that estimated by the Chang's method. But, as it is difficult to make it definite in what portion of a load-displacement curve the calculated spring constant should be corresponded to the slope, it is doubtful whether such a comparision with the calculated and measured values is justifiable or not.

Accordingly, as the spring constants the measured values

$\omega=2.55$t/cm or 20t/cm

$\mu=0.034$t/cm

will be used for the successive analysis. In addition to the evaluation, the ultimate bearing capacity and the maximum pulling resistance can be also taken as

$R_u=600$kg

$R_m=320$kg

The ultimate horizontal resistance of the coupled piles which will be estimated by the method of analysis without consideration upon bending becomes

$$T=320\times 2\times\sin 10^\circ=110\text{kg}$$

In fact, the horizontal force at the moment that the in-batter pile exhibits the maximum pulling resistance is 200kg as shown in the graph described before, and so, the present design method gives a result falling into the safe side by about 45%.

The percentage of share becomes

$$\rho=\frac{0.034\times\cos^2 10^\circ}{(2.55\sim 20)\times\sin^2 10^\circ+0.034\times\cos^2 10^\circ}\times 100=(31\sim 5)\%$$

by substituting the spring constants ω and μ into Eq.5, where both the axial spring constants are assumed to be the same. This value corresponds to a flat line before an abrupt increase begins in Fig.39. The curve representing the percentage of share after that point is established with the same spring constants, but it results in disagreement. This seems to be caused by the fact that, as described before, the behavior of the the members of the coupled piles is different from that of a single pile and, furthermore, the axial resistance both downward and upward are assumed to be constant after the maximum pulling resistance in this calculation.

For comparision with the test results, the percentage of share, the vertical and horizontal displacement at the intersection of the model coupled piles are calculated by the new method of computation and plotted in the corresponding graphs, and how

reasonable estimation for coupled piles can be made on the basis of the realistic data will be illustrated. This method can be considered as a general procedure by which the more accurate answer can be deduced by using the informations without any hypothesis.

7 Acknowledgement

The series of tests on the model coupled piles subjected to a horizontal force had been undertaken and carried out since more than ten years ago under the instructions by the late Dr. K. Kubo. Then, Mr. F. Saegusa and Mr. A. Suzuki endevoured to analyze and made ready for publishing the test results. But unfortunately they were transfered to the other positions before its completion.

The author continued further additional tests to establish the new method of computation for design of coupled piles. His conclusion is attributed to the previous test results in a part, so he expresses his many thanks to Dr. K. Kubo, together with Mr. Saegusa and Mr. Suzuki, and to Dr. R. Yamamoto, the Director, who gave many suggestions to this paper. Finally, he is also grateful to Mr. M. Miyamoto, Mr. Y. Tanaka, and Mr. T. Takeda who helped his experiments and computed the data.

Appendix

1 Existing Data of the Load Tests on Coupled Piles in the Fields.

The outline of some existing data of load tests on coupled piles in the work fields of our country will be described in this chapter.

These data may not be useful for verification of the new method of computation, but for mere apprehension of the lateral behavior of the actually used coupled piles, because they consists of a more general type of coupled piles such as makes it impossible to use the new method of computation. However, the individual piles seem to have common features on their axial and lateral movement between the model and the actually used coupled piles, so that this description will be expected to be useful for further apprehension of the results of the model test.

1.1 A lateral load test on cast-in-place concrete piles (Kyoryo to Kiso 2)

Two cast-in-place concrete piles 1270mm in diameter and 39m in length were formed in the vertical 3.50m apart center to center. The top of each pile was connected by a concrete block. The bottom surface of the block was in contact with the ground surface and, a horizontal load was applied 30cm at height.

The test ground, was composed of alternating layers containing sandy and clay soils. The N value in sandy soil was 20 to 30, and in clay it was about 10. The unconfined compression strength increased with the depth, that is, from 1 to 2.5kg/

Note; this Appendix includes many references written by Japanese. The auther should make an excuse in translation into English at his own discrection.

cm^2 within the level of about -4.00m and -17.00m.

The result of a lateral load test on a single vertical pile in the same site showed that the coefficient of horizontal subgrade reaction decreased from $10kg/cm^3$ to $4kg/cm^3$ as the lateral deflection increased. Thus, to estimate the relations between a lateral load and displacement, rotation, axial forces, and bending moment in the piles, the value of a coefficient corresponding to the deflection of the coupled piles was presumed.

As a result, the two following items were concluded;

1) The axial and lateral spring constants within the range of an applied load were larger than expected.
2) The computation of the coupled piles showed the fact the result was slightly overestimated if the lateral spring constant estimated by a single pile test corresponding to the same deflection was used.

1.2 The result of a load test on steel piles in clay soil and the mechanism of the axial and lateral resistance (Kyoryo to Kiso 6, 7, and 8)

Two vertical and two batter piles making an angle 10° with the vertical, whose diameter, length, and thickness were 609.6mm, 27,700mm, and 12.7mm, were each connected at the tops 1570mm apart at intervals. The height of load application was 500mm.

The soil profile of the test ground was followed; the upper layer from the ground surface to -10m had 200 to 800% at water content, 0.15 to $0.35kg/cm^3$ at the unconfined compression strength, 4 to $10kg/cm^2$ at the modulus of elasticity of soil obtained by a pressiometer, 1.01 to $1.15g/cm^3$ at the unit weight, and 4 to 14 at void ratio.

In general inspection, this upper layer was rather compressible, consisting of almost uniform soil, and was fragile in horizontal pressure. Below this deposit, sandy clay containing gravels, which was compressed to some degree, was stratified until -15m. The N value of this layer varied from 3 to 14, the water content from 40 to 70%, the unconfined compression strength from 0.6 to $1.0kg/cm^2$, and the modulus of elasticity from 20 to $40kg/cm^3$.

At a depth of -15m, a soil layer 4m in thickness was encountered, consisting of a medium stiff diluvial deposit which contained sandy fraction as much as 56%. The N value varied from 10 to 25, the water content was about 80%, the unconfined compression strength $2.8kg/cm^2$, and the modulus of elasticity $120kg/cm^2$.

From -19m to -27m, the stratum consisted of sandy clay containing gravel which had been comparatively solidified. The N value varied from 10 to 30, the water content from 40 to 60%, the unconfined compression strength was $1.7kg/cm^2$ and the modulus of ealsticity $300kg/cm^2$.

A load and displacement diagram as the result of a load test on the same size of pile in the same site is illustrated in Fig.42. This graph shows that the tendency of settlement at downward loading was the same as that at a pulling test in so far as an open-ended pile was tested, and that the axial spring constant was about 250t/m as an average slope.

Furthermore, a lateral load test was carried out, where the height of load application was 200mm, and the most reliable one of load and displacement relationships was illustrated in Fig.43. Though this relationship is obviously represented in a curve which it is difficult to replace a spring constant with, about 2 t/cm might be taken

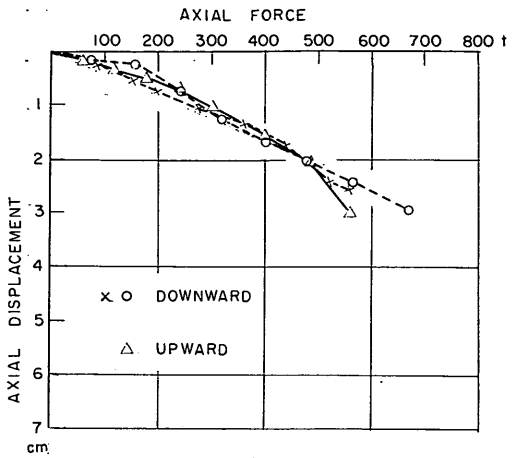

Fig.42 Axial force and displacement curve of a snigle pile

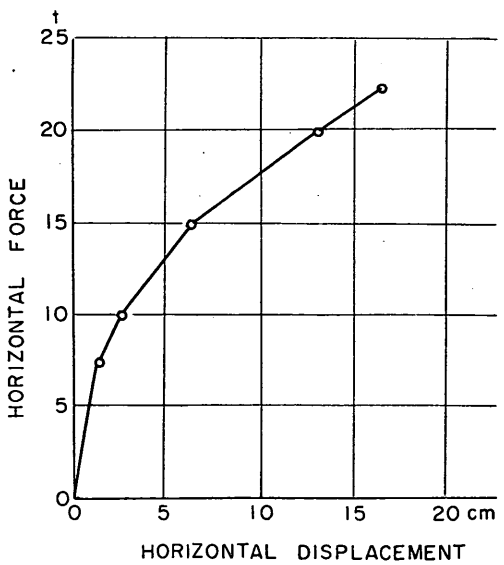

Fig.43 Horizontal force and displacement curve of a single pile

on an average value as shown by a straight line in the graph.

Strain gauges were attached on the sides of the piles gave the coefficient of horizontal subgrade reactions which varied with both the deflection and the depth. The average values along the whole length were 0.5kg/cm³ at 7.5tons, 0.2kg/cm³ at 10 tons, 0.15kg/cm³ at 15 tons, and 0.1 kg/cm³ at 20 tons. The relation between a horizontal load and displacement at the top of each coupled piles were illustrated in

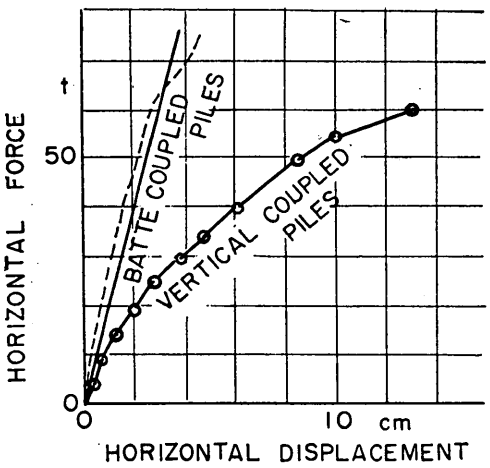

Fig.44 Horizontal force and displacement curve of coupled piles

Fig.44.

Though these phenomena were explained analytically by using the Z. Radosary-jevic's method, which is one of the methods of computation with consideration upon the bending resistance, the three moduli of elasticity obtained from the relations between a load and displacement, inclination, and fixed moment at the top respectively were different.

This report concluded that this difference was caused by the assumption that the soil would behave as elastic.

1.3 The report concerning a laterally loading test on coupled piles (Soil and Foundation 13-3)

The location for the test was in the Shiroyama district, where the ground was occupied by such soft clay as the N value was almost zero until the depth of 10 m. Below the upperlayer,there was a sandy stratum of which the thickness was about 5 m and the N value was more than 70. The unconfined compression strength in the most upper layer was 0.17 kg/cm^2 on an average.

The coupled piles for test was made of reinforced concrete, the diameter being 45 cm and the length 15 m. One concrete footing of which the bottom was situated 20mm at height above the ground surface was in a square shape at the plan, and connected each batter pile under the four corners symmetrically with respect to the center of the square footing. This batter was made at an angle of 12°30′ with the vertical, which was equalized to 9° from the side point of view. And the distance between the two tops of the piles from the side view was 1.20m

Another concrete footing were supported by six vertical piles.

Apart from these coupled piles, three single vertical piles were driven to carry out the axial load, lateral load, and pulling tests respectively. The height of lateral

load application was 43cm, and the load and displacement relationship at the height of 45cm was illustrated in Fig.45. From this graph a lateral spring constant seemed to be 2t/cm.

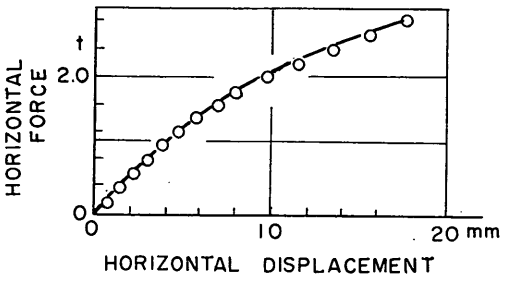

Fig.45 Horizontal force and displacement curve of a single pile

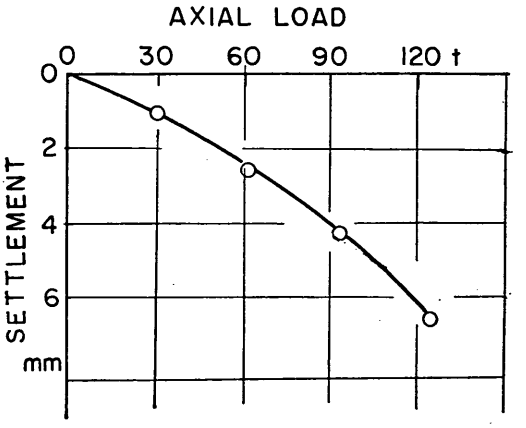

Fig.46 Axial force and displacement curve of a single pile

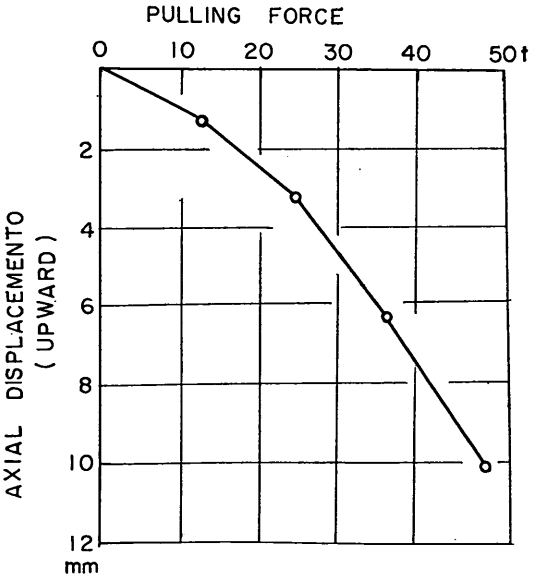

Fig.47 Horizontal force and displacement curve of a single pile

The results of the axial load and pulling tests were also shown in Fig.46 and Fig.47, where these curves are constructed by tracing on the virgin curves of a cyclic load test. The axial spring constants were 200t/cm on downward loading and 60t/cm on pulling.

The horizontal load tests on each footing were carried out under four conditions;

that is, the first with crushed gravels and the second with Kanto loam backfilled against the footing, the third with a surcharge of 85 tons by total weight on the footing and the fourth without any surcharge. The horizontal displacement, vertical displacement, and rotation against a horizontal load under the last condition were written as in Fig.48 to Fig.50.

As a result, the followings were concluded;

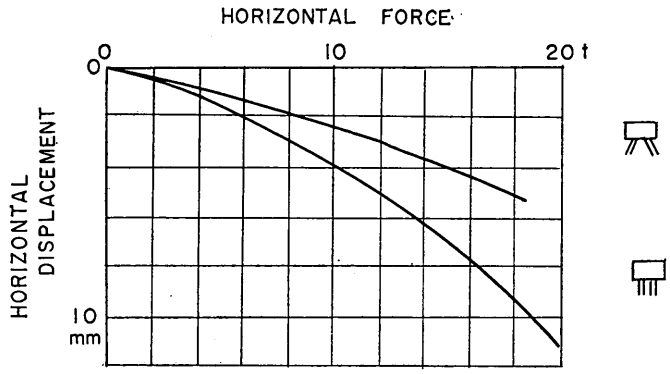

Fig.48 Horizontal force and displacement curve of coupled piles

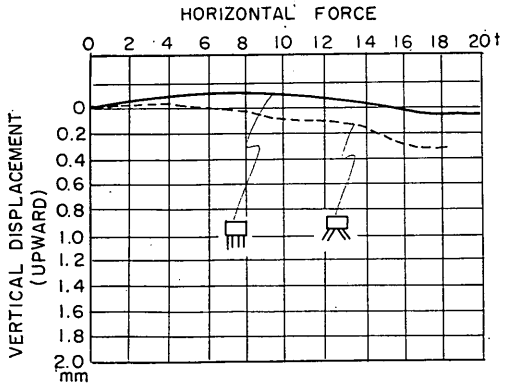

Fig.49 Horizontal force and vertical displacement curve

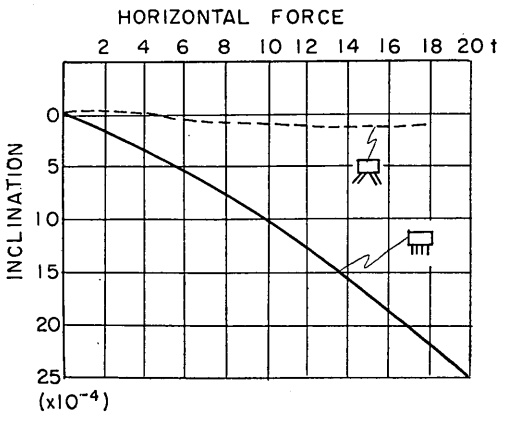

Fig.50 Horizontal force and rotation curve

1) The displacement of the footings under a horizontal load was scarcely affected by the surcharge.
2) The stress occured in the piles was the sum of bending stress which could be approximately calculated by an elastic beam method and axial stress caused by a rotation of the footing.

Though there are other many items of conclusion than the above-mentioned, only items are written here which will be useful directly to the investigation about the

model test results.

1.4 Foundation works in the Shin Ishikari Bridge (Soil and Foundation 13-8)

Test piles were driven into such ground as follows; the uppermost layer was about 18m thick and consisted of silt and sand, whose N value varied from 10 to 20, and its coefficient of horizontal subgrade reaction obtained by means of a pressiometer was 1.31kg/cm³ on an average. Below this deposit, silty clay was encountered until elevation -35m. The N value and two unconfined compression strength of this soil were about 10 and one less than 0.20t/m² and another about 1.0kg/cm². Below elevation -35m, sand and gravel underlay of which the N value was more than 10 to 50.

Three kinds of pile tests were carried out; an axial and two lateral load tests on the coupled piles. In Fig. 51, only virgin potion of the load and settlement curves in the axial load test was illustrated. The spring constant could be assumed to be 300t/cm from this graph. This reporter expressed this curve mathematically as $\delta=0.0015\times N^{1.53}$, where δ was the total settlement (mm) and N was the load intensity (ton).

A load and displacement diagram as the result of a horizontal load test on a single out-batter pile making at an angle 12.5° with the vertical was shown in Fig. 52. The spring constant could be assumed to be about 15t/cm from this graph.

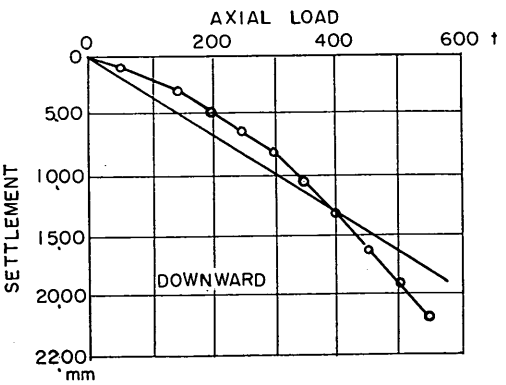

Fig. 51 Load and settlement curve of a single pile

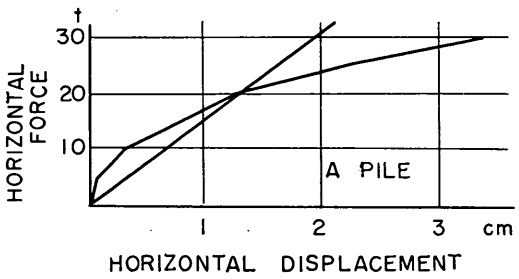

Fig. 52 Horizontal force and displacement curve of a single pile

And then, the same relationship with respect to the coupled piles battered at an angle 12.5° towards each other pile, having a distance of 3.92cm between each top of the piles connected by a concrete block that was situated closly to the ground surface, was shown in Fig.53.

Fig. 54 showed a rotation of the concrete block with respect to the load direction.

In this report, the repoter proposed a formulation of a spring constant of coupled piles as

$$K=\frac{2(r\cos\theta+1/k_0\sin\theta)}{r/k_0} \qquad (13)$$

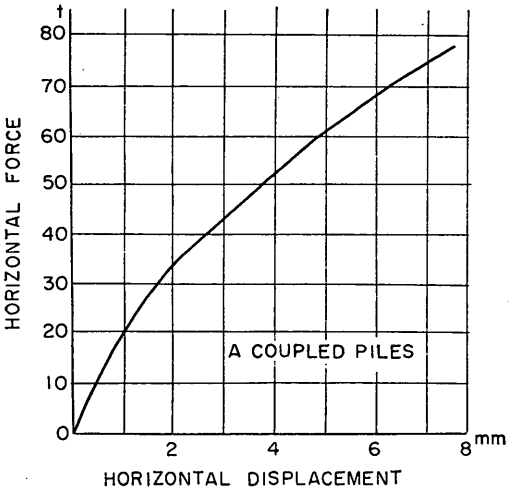

Fig.53 Horizontal force and displacement curve of coupled piles

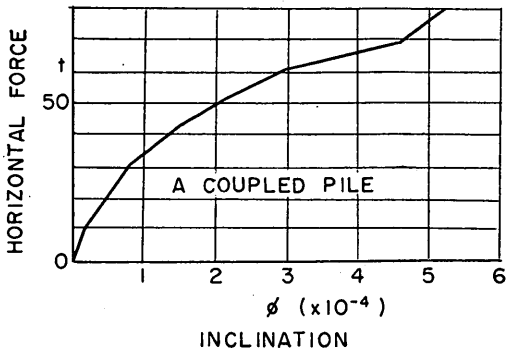

Fig.54 Horizontal force and rotation curve of coupled piles

where $k_0=2EI\beta^3$, r$=L/E$, EI is flexural rigidity of a pile, β relative stiffness (see symbols) θ angle of batter, L the length of a pile, and E the Young's modulus of a pile materal.

1.5 Driving tests and a lateral load test on long batter piles

Coupled piles and the two uncoupled batter piles were tested under a horizontal load. Test ground was consisted of an upper layer being 8m in thickness composed of fine sand, an intermediate layer being 35m in thickness of silty clay, and an underlying layer of sandy gravels. The N value of the upper layer was about 10. The coefficient of horizontal subgrade reaction increased from 0.7kg/cm³ at eaevation -10m to 3.5kg/cm³ at elevation -40m.

The test pile was a steel pipe that had 485mm in external diameter, 9mm in thickness, and 51m in length. The inclination of each pile was made at the angle 11°30′ with the vertical, the distance between the tops of cach pile was 60cm, and the unsuported length was 2.4m. The height of load application was 4m 26.

The relation between a lateral load and displacement were as shown in Fig.55. Fig.56 and Fig.57 were with respect to the out-batter pile and the in-batter pile. To show how much percentage of share occured in the coupled piles, the check at 39 ton load intensity, for example, gave only 6.2 to 6.4% because the part resisted by the axial resistance amounted as much as 36.6 tons.

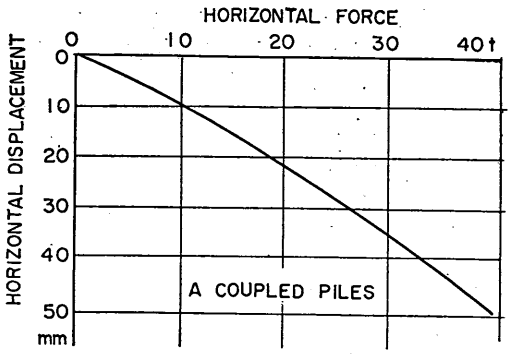

Fig.55 Horizontal force and displacement curve of coupled piles

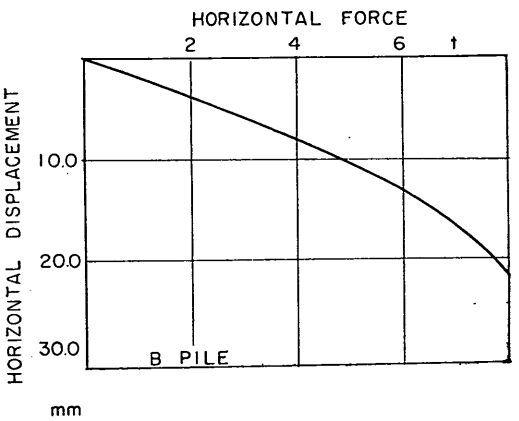

Fig.56 Horizontal force and displacement curve of an out-batter pile

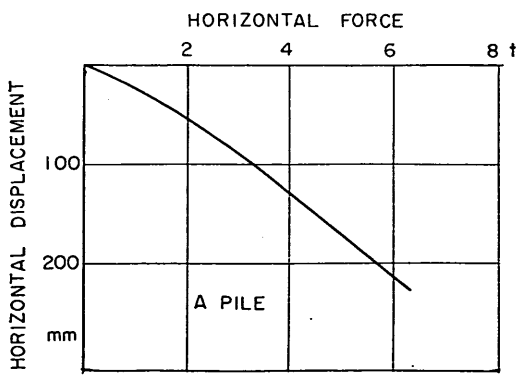

Fig.57 Horizontal force and displacement curve of an in-batter pile

1.6 Load tests on a steel pile at the Shin Yoshinogawa Bridge

The ground consisted of a sandy deposit with 15m thickness, and the N value was about 10. From elevation -15m to elevation -25m there was a silty clay layer whose N value was only 0 to 5. At the deapest, sand and gravel were situated whose N value was more than 50.

Coupled piles were composed of two piles with 37.5m in length, and 101.6cm and 81.28cm in diameter, of which the tops were connected 2.5m apart. The inclination was each made at the angle 8° with the vertical. The horizontal load tests on two single piles were carried out before on the coupled piles. The kind of piles for test was two.

The displacement of the single pile at elevation 50cm above the ground was plotted on the same diagram against the horizontal force as that of the coupled piles was (Fig. 58). But the height of load application on the coupled piles was 100 cm. The spring constants obtained from this graph were about 8 t/cm for a pile with 18.28cm in dia. and about 20 t/cm with 101.6cm in dia. on an average. Besides

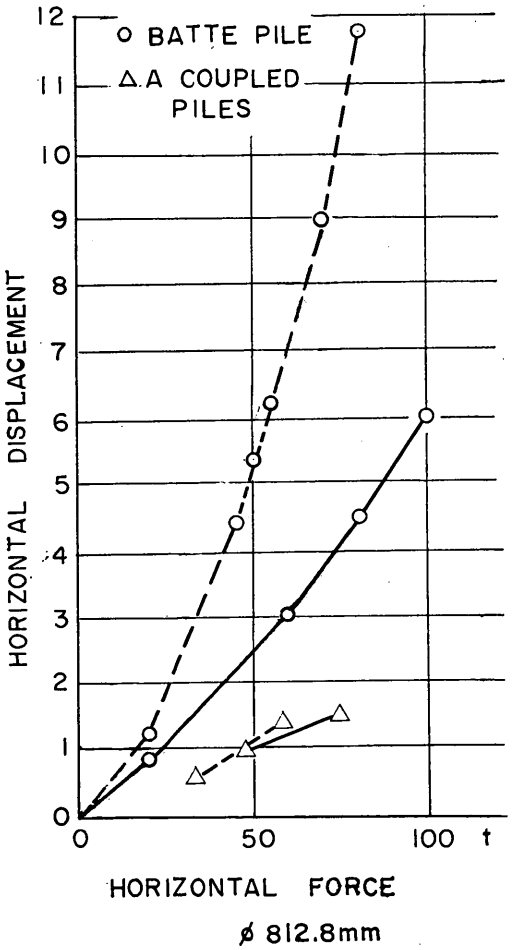

Fig.58 Horizontal force and displacement curve of a single pile and coupled piles

these tests, the spring constant with regard to the single pile and the coupled piles which were resulted from the other horizontal load tests were collected as shown in Tab.5.

Tab.5 Data of spring constants

TESTING SITE		LATERAL SPRING CONSTANT		NOTICE
		SINGLE PILE	COUPLED PILES	
THE SHIN-KASAI BRIDGE		VERTICAL : 18t/cm BATTER : 20t/cm	50t/cm	ϕ=450 l=47m VERTICAL PILE AND BATTER PILE (10°)
KAKUYAMA BRIDGE		VERTICAL BATTER vague	FIVE TIMES A SINGLE PILE	ϕ=500 VERTICAL PILE AND BATTER PILE (12.5°)
MEMANBETSU BRIDGE		BATTER : 1.5t/cm	18t/cm	ϕ500 TWO BATTER PILES (15°) l=39m
THE SHIN-YOSHINO RIVER	ϕ800 HORIZONTALLY LOADING	20t/cm	45t/cm	l=37.5m ANGLE OF BATTER 8°
	ϕ800 HORIZONTALLY AND VERTICALLY LOADING	20t/cm	65t/cm	DITTO V=200t T=70t
	ϕ1000 HORIZONTALLY LOADING	25t/cm	50t/cm	DITTO
	ϕ1000 HORIZONTALLY AND VERTICALLY LOADING	25t/cm	65t/cm	DITTO V=400t T=100t

1.7 On the breakwater at the Nishinomiya Port and laterally loading tests

The soil profile was such as; silt covered the surface from elevation -5.50m, which corresponded to the level of the sea bottom, to elevation -13.70m. Until elevation -17.50m below this deposit, a silty sand layer was encountered.

The in-batter pile was H-section pile with dimensions of 294×302×12×12×19.00, making at an angle 5° with the vertical, and the out-batter pile was a steel pile with 457.2cm in diameter, making at an angle 15° with the vertical. Both piles were installed into the silty sand. The tops of the piles were located at higher elevation than the water level by 8m, connected by a concrete block having 3.00m in width. The coefficients of horizontal subgrade reaction obtained by a pressiometer were 0.23 kg/cm^3 for the H-section pile, and 0.15kg/cm^3 for the pipe pile.

The number of tests was five; that is, twice in slowly loading tests on the coupled piles equipped with and without a strut bar near the middle height above the

sea bottom respectively, and once in a repeatedly loading test on the ones with a strut bar.

The result showed the fact that the upper concrete block was rotated with an increase in a horizontal load; the side supported by the pipe pile going upward and the other side downward. The shearing stress, inclination, and deflection of the coupled piles were obtained by strain gauges attached on the sides of the piles. The results is shown in Tab. 6. Additionally, the percentage of share was calculated by using the above results. As a result, it was about 0.37.

Tab. 6 Results of loading tests

TEST		1	2	3	4	5
LOADING		SLOWLY	SLOWLY	RAPIDLY AND RE-PEATEDLY	SLOWLY	SLOWLY
STRUT BAR		WITH	WITH	WITH	WITHOUT	WITHOUT
MAXIMUM LOAD (t)		9.60	17.28	9.60	9.60	17.28
MAXIMUM DISPLACEMENT(cm)		2.75～3.00	4.75～5.00	3.20～4.40	4.00～4.10	5.60～6.25
RESIDUAL DEFORMATION (cm)		0	1.50	2.50	2.50	2.50
ROTATION OF A SLAB (〃)	DIRECTION OF LOADING	420	850	—	460	910
	PERPEN-DICULAR TO LOADING	230	750	—	630	1000
AXIAL FORCE(t)	PIPE	14	29	11	8～20	21～41
	H-SECTION	20	25	10	10	21
BENDING MOMENT (t-m)	PIPE	11.0	22.5	11.0	11.3	21.2
	H-SECTION	8.5	16.5	8.8	9.4	18.8
SHEARING FORCE (t)	PIPE	1.9	3.8	1.8	1.9	3.4
	H-SECTION	1.4	3.0	1.75	1.9	3.5

On the basis of the test results, this reporter proposed a method of computation on coupled piles; a pseudo-fixed point in a pile subjected to a lateral force might be assumed by adopting relative stiffness β (see symbols), and the upper part above that fixed point was assumed to be a rigid-frame structure. Usually that fixed point is assumed to be located at the depth of $1/\beta$ below the ground level, and then the shearing force at the top of the piles subjected to a horizontal force T at the upper block are reepectively

$$H_1=\frac{T}{(2+\alpha)(k+1)}$$

$$H_2=\frac{2kT}{(2+\alpha)(k+1)} \qquad (14)$$

where k is the ratio of the flexural rigidity of an out-batter pile to that of an in-batter pile, and

$$\alpha=\frac{L_5+L_4}{L_3} \tag{15}$$

in which L_3, L_4, and L_5 are the length shown in Fig. 59.

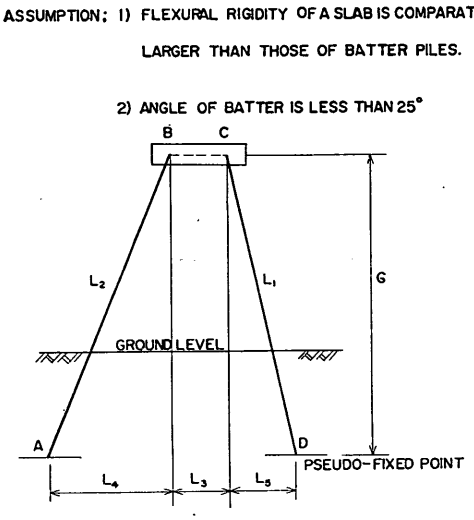

Fig.59 Illustration of L_3, L_4, and L_5

By substituting with the above into the following equations

$$\left.\begin{aligned} N_1&=\frac{V\sin\theta_2-T'\cos\theta_2}{\sin(\theta_1+\theta_2)}\\ N_2&=\frac{V\sin\theta_1+T'\cos\theta_1}{\sin(\theta_1+\theta_2)}\end{aligned}\right\} \tag{16}$$

the axial forces acting at the tops are calculated, where $T'=T-H_1-H_2$, V is a vertical force, and θ_1 and θ_2 are the angles of in-batter and out-batter. By using the above equations, the values with respect to the coupled piles without a strut bar were obtained as shown in Tab. 6.

In that table the percentage of share calculated on the basis of the analytical method can be compared with the measured ones. As a result, the calculated value 0.43 is higher than the measured one by about 16%.

Heretofore, the results of the horizontal load tests carried out at several field locations have been described together with the soil conditions at the testing site. Most of these coupled piles are composed of such piles as connected by a concrete block at some interval apart. Among them there are such coupled piles as composed of vertical piles only.

Therefore, it may be necessary to note a substantial difference in structural mechanism between such coupled piles and the model ones for test in the laboratory which were composed of two intersecting batter piles hinged or fixed at one point.

For instance, if such a type of coupled piles as tested in the fields are hinged at

the connections, a whole horizontal force could be resisted by the bending only; the percentage of share becomes always to be unity. On the other hand, the simplest type of coupled piles such as tested in the laboratory can not take unity even though it may be hinged.

This is caused by the allowance for vertically slipping in each top of the piles. It may be derived from this consideration that the percentage of share is higher in the simplest type of coupled piles than the ones with some interval at their tops even though both are connected in rigidity.

Therefore, the later might be distinguished by naming "coupled piles with a footing"

2. On Load-Displacement Relationships of a Pile

2.1 Axial movement

A design method of coupled piles with consideration upon the bending resistance demands a well-defined meanchism of axial movement. It is indispensable to know it for an estimation of the horizontal behavior of coupled piles under a certain applied

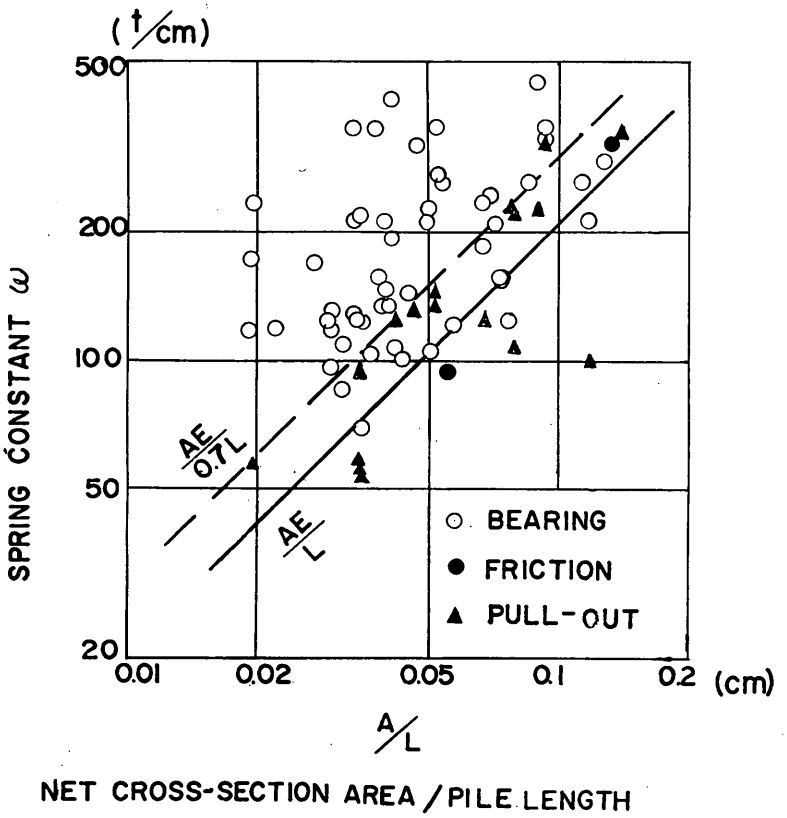

Fig.60 Data of axial spring constants obtained by load tests in many fields

force, although the axial spring constant pertarning to a single pile has only to be known in the existing methods with consideration upon the bending resistance.

Analytical study on the mechanism of axial displacement, that is, settlement and rise at the top of a pile has been much belated in comparision with that of lateral movement. Therefore, it is necessary to collect as many data as possibly from the load tests or the observed settlement of a building founded on piles for its statistical treatment. Fig. 60 shows the correlation between the axial spring constants and the pile size ratio A_p/L which was obtained from many results of the load tests carried out at the building sites.

Because the axial resistance of a pile consists of two elements, point bearing and skin friction, by which the share of attribution will vary accordingly to the soil conditions, the load intensity, the rate of loading, and the dimensions of a pile, it is very difficult to glasp a definite relation between the load and displacement.

The expression for this relationship which is said to be in the highest accuracy is

$$N_a=R_u\ (1-e^{c\delta}) \tag{17}$$

where R_u is the ultimate bearing capacity, N_a and δ are the axial force and settlement, and c is a constant. This expression will be adaptable beyond the ultimate bearing capacity only if the value of c is changed. This constant is a function of the loading duration and of number of repeatedly loading. But c might not be given as a definite figure.

Considering its linear relationship when plotted in a double logarithmic scale as seen in the results of a load test, it can be also considered to be expressed such as

$$N_a=d\delta^n \tag{18}$$

where n and d are constants, the latter being dependent upon the loading duration.

Fujita, who has studied that relationship with respect to 100 cases of steel pipe piles and 40 cases of H-section piles, reported that n had a range from 0.6 to 0.8

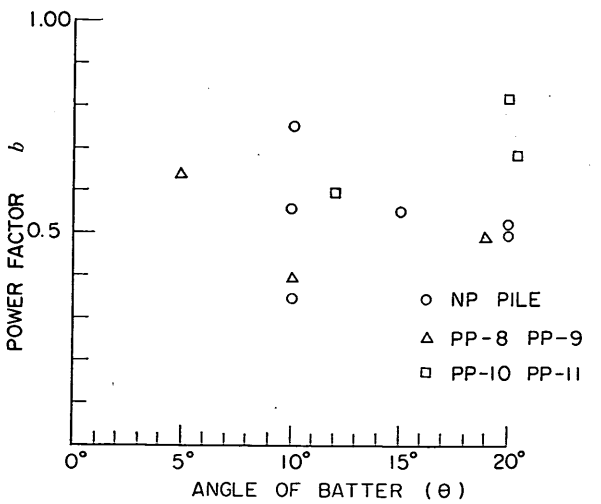

Fig.61 b values against angle of batter

and d was dependent upon the N value at the ground.

As stated in Chap.4, the relation between the axial force and displacement plotted in Fig.36 was expressed as a straight line on a double logarithmic scale, and so this case can be also expressed as Eq.18 or, as a converse form,

$$\delta = aN_a^b \tag{19}$$

where a and b are constants. These may perhaps be dependent upon both piles and soil conditions, and are plotted against the angle of batter as shown in Fig. 61 and

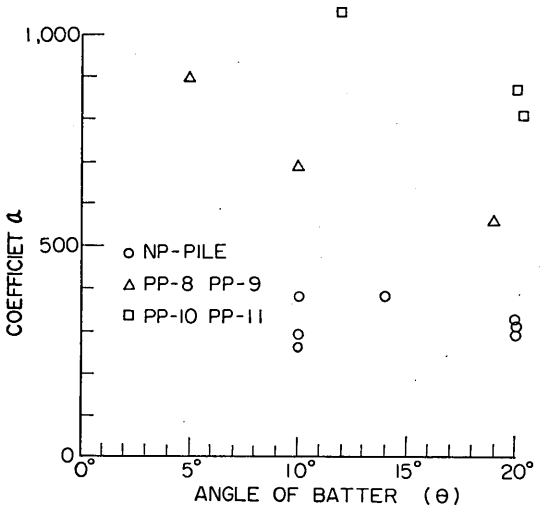

Fig. 62 a values against angle of batter

62, for the soil conditions through all series were controlled in almost the same way and the effect of the angle of batter as piles conditions only was prominant.

As a result, it seems rather difficult to find out a distinct tendency, but b increases somewhat as the angle of batter increases. This may be due to the reason that a pile with a larger angle of batter has smaller bearing capacity, because its point is set at less depth. Smaller bearing capacity means the earlier changing to a plastic state of the bearing stratum. Thus, the soil supporting such a pile fails at an early stage of loading than the one with a smaller angle of batter.

Saying regarding a load-settlement or a pull-rise curve where b decreases as a load or pull increases in general, the movement of the latter pile may remain at the early part of such a curve, which means b is larger, and on the other hand, the movement of the former pile may go on the advanced stage of such a curve, which means b is smaller.

Next, a decreases as the angle of batter increases respectively. This seems to be caused by the fact that a pile with a smaller angle of batter will increase in its bearing capacity due to its larger deflection.

Kézdi, using a relation between shearing stress and strain measured by a direct shear test on sand, gave such a formula as

$$N_a = K_0 \, \gamma \, A_s \tan \Phi \frac{l^2}{2}\left[1-exp\left(-f\frac{\delta}{\delta_{max}-\delta}\right)\right] \tag{20}$$

where N_a ; axial force
K_0 ; coefficient of easth pressure at rest
γ ; unit weight of soil
A_s ; peripheral length of a pile
f ; constant
Φ ; angle of internal friction
l ; embedded length
δ ; settlement
δ_{max} ; final settlement

Kitajima reported that n in Eq.18 became about 1.5 and d was equal to $\delta_{max}/N_u^{1.5}$ for a load beyond half the ultimate bearing capacity, on the basie of the results of the load tests carried at many locations on steel piles and concrete piles whose points were set into sandy or clay layers.

When the above-mentioned expressions are applicable to the existing method of computation with consideration upon the bending resistance, it will be necessary to establish a procedure to determine the most suitable modulus to express the behavior of coupled piles as an axial spring constant. Sometimes an initial modulus of these curves may be adopted because the axial movement of each member of coupled piles subjected to a horizontal force is to a little extent limited.

But, in this paper it will be more interesting to take a secant modulus, for example, of a slope passing through a point of one-half the ultimate bearing capacity, because the answer obtained by the existing methods using such a spring constant can be compared with the one obtained by the new method which can cover a wide range of horizontal behavior of coupled piles.

Therefore, using such a secant modulus as stated above, ω will be expressed from Eq.18 as

$$\omega_{50}=0.72dR_u \tag{21}$$

A standard manual of design in substructure of a bridge in Japan specifies a spring constant similar to the above equation such as

$$\omega=0.4R_u \text{ (t/m)} \tag{22}$$

Thus, such a spring constant can be estimated without carring out any load test, if the ultimate bearing capacity estimated by some pile formula is substituted into the above equations.

Furthermore, the same standard manual gives an equation for an estimation of a spring constant with the use of the N value or a coefficient of subgrade reaction at the bearing stratum. But this is rather complicated.

Yokoyama, assuming that a pile is compressed in all or a part of its length accordingly as a point-bearing or a friction pile, gave an equation such as

$$\omega=\frac{A_pE}{\lambda+\nu L} \tag{23}$$

where A_p ; cross-sectional area of a pile
E ; Young's modulus of a pile
λ ; unsupported length of a pile
ν ;
$\begin{cases} 1 & \text{for a point-bearing pile} \\ 1/3 & \text{for a friction pile driven into clay} \\ 8/15 & \text{for a friction pile driven into sand} \end{cases}$

In any event, these spring constants can be used only for the range of unyielding state and yet that of a tension pile has scarcely been unknown.

2.2 Lateral movement

The question in the lateral behavior of members of coupled piles has been found out to be almost the same as that in a single pile. Accordingly, a method of analysis on a laterally loaded pile may be applicable to the calculation on coupled piles. The fact that the lateral behavior of a batter pile of coupled piles subjected to a horizontal force can be considered to be the same as in the case of a single pile had been also certified in the laboratory. However, there remains a problem what difference between a single pile and coupled piles will be brought out by the fixty at the top.

To estimate the behavior of coupled piles as accurately as possible, it is necessary to use the procedure by which the lateral behavior of a single pile can be analyzed as scrupulously as possible. Simultaneously the revisal procedure which is as minute as possibly will be demanded.

At present, the most familiar method of computation on a lateral behavior of a single pile is the Chang's method, which assumes that soil reaction varies in linear proportion to the deflection of a pile embedded into uniform soil along its depth. An assumption of linearity in soil reaction turns out to express the linear behavior of a pile, and especially the lateral movement of a pile head becomes in linearity, which corresponds directly to a lateral spring constant, and so only the expressions for it will be presented; in the case of a free-head pile,

$$\left.\begin{aligned} \mu &= \frac{E_s}{2\beta} && \text{for a pile without unsupported length} \\ \mu &= \frac{3EI}{\lambda^3 \psi(\beta\lambda)} && \text{for a pile with unsupported length} \end{aligned}\right\} \quad (24)$$

and in the case of a fixed-head pile

$$\left.\begin{aligned} \mu &= \frac{E_s}{\beta} && \text{for a pile without unsupported length} \\ \mu &= \frac{12EI}{\lambda^3 \bar{\psi}(\beta\lambda)} && \text{for a pile with unsupported length} \end{aligned}\right\} \quad (25)$$

where

$$\psi(\beta\lambda) = \frac{(1+\beta\lambda)^3 + 1/2}{(\beta\lambda)^3} \qquad \bar{\psi}(\beta\lambda) = \frac{(1+\beta\lambda)^3 + 2}{(\beta\lambda)^3} \quad (26)$$

β ; (see symbols)
E_s ; modulus of elasticity of soil
EI ; flexural rigidity of a pile
λ ; unsupported length

Besides the Chang's method, a lateral spring constant can be estimated by the Matlock and Reese's method which assumes that there is a variation of a coefficient of horizontal subgrade reaction with the depth. The procedure of computation for use is explained in detail, for example, by Takeshita, who dealt with an analytical treatment of coupled piles on the basis of the above-mentioned estimation method.

Fig.63 shows the correlation between the lateral spring constants and the factor of pile condition which was collected from the results of many laterally loading tests.

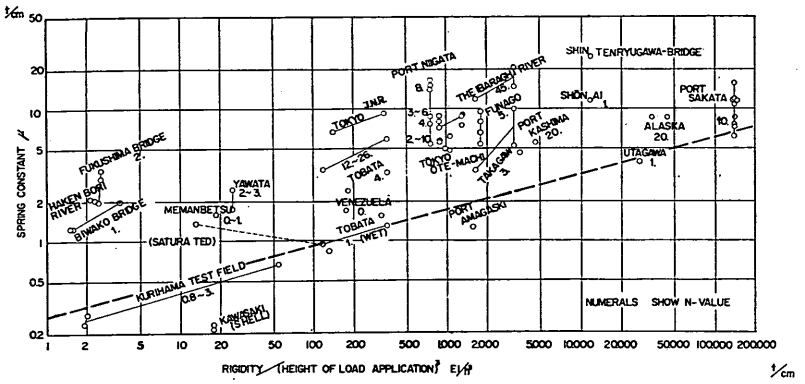

Fig. 63 Data of lateral spring constants obtained by load tests in many fields

Finally, the Kubo's method which can give the most reliable imformation regarding the lateral behavior of a single pile can be refered to the previously presented papers on its practical use for the new method of computation on coupled piles. As its content is so voluminous that the present paper could not help dealing with it in conception, not in detail so as to its use in the new method.

The auther wishs that one who has an intention of its practical use for the new method would see Ref.15.

Reference

1) Study on Lateral Resistance of Steel Piles (No. 1); 1966, Japan Soc. of Soil and Found. Eng..
2) Nishikawa, Ishii, Shima, Kato; On the Breakwater at the Nishinomiya Port and Laterally Loaded Tests; 11th Discussion Meeting on Japan Port Construction Works, 1965, Port and Harbour Bureau.
3) Takahashi, Aoki; A Lateral Load Test on Cast-in-Place Concrete Piles; Kyoryo to Kiso, No. 2, 1968.
4) Akai; The Results of Load Tests on Steel Piles in Clayey Soil and the Mechanism of Axial and Lateral Resistance; Kyoryo to Kiso, No. 6, 7 and 8, 1968.
5) Matsumoto, Tsuchiya, Sugino; The Report Concerning a Laterally Loading Test on Coupled Piles; Soil and Found. Eng., 13-3, 13-4, 1965.
6) Takahashi; Foundation Works in the Shin Ishikari Bridge; Soil and Found. Eng., 13-8, 1965.
7) Standard of Design in Substructure of a Bridge, 1965.
8) Takeshita; Coumputation Method of Coupled Piles; Japan Civil Eng., Vol. 19 No. 8, 9 and 10, 1964.
9) Yoshimura, Ishiyama, Nishitani, Yoshida; Load Test on a Steel Pile at the Shin Yoshinogawa Bridge; Note of Civil Eng., Japan Soc. of Construction Works, 7-7, 1965.
10) Standard Manual on Design of Steel Pile Foundation of a Building; Japan Soc. of Arch., 1964.
11) Yokoyama; Design and Construction on Steel Pile; Sankaido, 1963.
12) Standard Manual on Port and Harbour Structures; Port and Harbour Bureau, 1964.
13) 3rd Discussion Meeting on Soil and Found. Eng.; Japan Soc. of Soil and Found. Eng.,

1969.
14) Shinohara, Kubo; Experimental Study on the Lateral Resistance of Piles; Report of Transp Tech. Res. Inst., Vol.11 No.6, 1961.
15) Kubo; A New Method for the Estimation of Lateral Resistance of Piles; Report of Port and Harbour Res. Inst., Vol.2 No.3, 1964.
16) Kitajima, Kakizaki, Hanaki, Tahara; On the Axially Bearing Capacity of Single Piles; Tech. Note of Port and Harbour Res. Inst., No.36, 1967.
17) Aoki; Ultimate Design of Coupled Piles (tentative title); unpublished.
18) Kawanishi; Generalized Ultimate Design of Coupled Piles (tentative title); unpublished.
19) Tateishi, Yoshimura; Driving Test and Lateral Load Test on Long Batter Piles; Proc of Harbour Engineering, No. 29, 1960.

Simbols

suffix 1; out-batter pile
suffix 2; in-batter pile
ρ ; percentage of share
H ; shearing force (lateral force) at the top of a pile
θ ; angles of batter of a batter pile
T ; horizontal force
N ; axial force at the top
δ ; axial displacement at the top
y_1 and y_2 ; deflection at the tops of the in-batter and the out-batter piles
y ; deflection of a pile
ω ; axial spring constant of the top
μ ; lateral spring constant of the top
K ; horizontal spring constant of coupled piles
Δ ; a remainder
ΔN_1; additional axial force of the in-batter pile
X ; vertical displacement of the intersection of couple piles
Y ; horizontal displacement of the intersection of coupled piles
B ; width of a pile
k ; a ratio of flexural rigidity of an out-batter pile to that of an in-batter pile
α; $(=\frac{L_4+L_5}{L_3})$
L_3, L_4, and L_5; the length as shown in Fig. 59
V ; vertical force
T' ; $(=T-H_1-H_2)$
c ; constant
d ; constant
n ; constant
a ; constant
b ; constant
K_0 ; coefficient of earth pressure at rest
γ ; unit weight of soil
Φ ; angle of internal friction of soil
l ; embedded length
f ; constant

δ_{max} ; final axial displacement
ω_{50} ; a 50% secant modulus of a load and displacement curve
EI ; flexural rigidity of a pile
l_{m1} ; the depth to first zero moment
$\bar{N}$; N value at a depth of 1m
N ; blow number of standard penetration test
k_s ; coefficient of soil reaction
p ; soil reaction
x ; depth
y ; deflection of a pile
R_m ; maximum pulling resistance of a pile
R_u ; ultimate bearing capacity of a pile
R_y ; yield value of a pile
A_p ; cross-sectional area of a pile
A_s ; peripheral area of a pile
$\overline{N}$; average N value along the embedment of a pile
r ; $(=L/E)$
L ; length of a pile
E ; Youngs' modulus of pile material
β ; relative stiffness $(=\sqrt[4]{k_hB/4EI})$
k_h ; coefficient of horizontal subgrade reaction
λ ; unsupported length of a pile
ν ; constant for different aspect of a pile
E_s ; modulus of elasticity of soil $(=k_hB)$
ψ ; a function of $\beta\lambda$
$\overline{\psi}$; a function of $\beta\lambda$
N_a ; axial force at the top of a single pile